A STUDY ON COMPLEXITY

A Thesis

presented to

the Faculty of Science

at the University of Cape Town

In Partial Fulfillment

of the Requirements for the Degree

Master of Science

---

by

DIMAKATSO RENEILWE RAPOTU

Dr. Haque, Thesis Supervisor

Professor Murugan, Thesis Co-Supervisor

FEBRUARY 2023

The undersigned, appointed by the dean of Science, have examined the thesis entitled

A STUDY ON COMPLEXITY

presented by Dimakatso Reneilwe Rapotu,
a candidate for the degree of Master of Science in Applied Mathematics,
and hereby certify that, in their opinion, it is worthy of acceptance.

Dr. Haque

Professor Jeff Murugan

Professor [Committee Name]

Professor [Committee Name]

Professor [Committee Name]

DEDICATION

To my beloved parents Shadrach and Sarah Rapotu, thank you for always being a fortress to establish dreams on and believing in me, my Trevor Noah of a sister Nelly, thank you for being my smile keeper, my biggest cheerleader and lifelong co-worker! and my care bear - my oldest sister Thabang thank you for being a dependable deputy parent that any sibling could ever hope for. To my antecedents that paved the path to my existence, your internal convictions and dreams still blossom today through us.

Ho Rara, Mmupi wa tsohle, ke lebohela moya wa hao.

ACKNOWLEDGEMENTS

I would like to thank Dr. Haque for being a supervisor that any student endeavouring into graduate school would need - his support, kind critique and guidance are traits that are crucial for supervisors that have a heart for developing new researchers. Professor Murugan, thank you for your hard work, for organising engaging seminars and workshops and for creating open spaces that only some of us could only have dreamt of entering.

My collaborators to whom I am indebted to - Ghadir Jafari and Pratik Nandy thank you for sparing your time, knowledge and effort towards the existence of this project.

The HePCat/QGasLab student group - to those whom I have personally met and also those I couldn't physically meet, the random memes, unfulfilled online meetings and helpful Q and A messages still afforded me some form of interaction, and for that, I am grateful.

Finally, my funders - The Council for Scientific and Industrial Research (CSIR), thank you for affording me this opportunity.

TABLE OF CONTENTS

ACKNOWLEDGEMENTS ii

LIST OF TABLES v

LIST OF ILLUSTRATIONS vii

ABSTRACT viii

1 INTRODUCTION 1

1.1 Background and Motivation . . . 1

1.2 Thesis Outline . . . 2

2 QUANTUM COMPLEXITY 3

2.1 Complexity . . . 3

2.2 Complexity in Holography . . . 5

2.3 Complexity in QFT . . . 10

2.3.1 Circuit complexity . . . 12

2.3.2 Fubini-Study complexity . . . 18

2.4 Krylov Complexity . . . 20

2.4.1 Krylov complexity through the two-point function . . . 26

2.4.2 Geometry of krylov complexity . . . 27

2.4.3 Growth of states in krylov basis . . . 31

3 COMPLEXITY FOR OPEN QUANTUM SYSTEMS 37

3.1 Introduction . . . 37

3.2 Krylov complexity . . . 39

3.3 Circuit complexity . . . 48

3.3.1 Complexity of purification . . . 48

3.3.2 Complexity by operator state mapping. 55
3.4 Krylov complexity for non gaussian random matrix model random matrix model with noise 57
3.4.1 The spectral form factor 57
3.4.2 Complexity Results 61

4 CONCLUSION **65**
4.1 Summary 65
4.2 Outlook 67

BIBLIOGRAPHY **74**

LIST OF TABLES

2.1 Lanczos algorithm 23

3.1 Equations of motions for different systems 40

3.2 Arnoldi iteration algorithm 40

3.3 Mapping of a krylov complexity to a particle hopping in a half - infinite chain 45

LIST OF ILLUSTRATIONS

2.1 Quantum circuit model example. Retrieved from [1]. 4

2.2 Generalized features of computational complexity for a chaotic Hamiltonian. Retrieved from [2]. 5

2.3 AdS/CFT correspondence. Retrieved from [3]. 5

2.4 Penrose diagram of schwarzchild geometry. Retrieved from [4] 7

2.5 Complexity = volume for eternal AdS black hole (left) and complexity = action (right). Retrieved from [5]. 8

2.6 Multi-scale entanglement renormalization ansatz. Retrieved from [6]. 9

2.7 pictorial representation of geodesic corresponding to the complexity through circuit complexity metric. Retrieved from [5]. 16

2.8 Pictorial representation of geodesic (blue) corresponding to the complexity through Fubini-study metric between ψ_R and ψ_T. Retrieved from [7]. 19

2.9 Lanczos sequences for L = 8, 9, 10 in linear (left) and logarithmic (right) scale along the horizontal axis. Retrieved from [8]. 25

2.10 Comparison of K-complexity for L = 8, 9, 10 for exponentially long times (left) and for early times (right). Retrieved from [8]. 26

2.11 Spectral function $\Phi(\omega)$(above) and analytical function of correlation function $C(t)$. Retrieved from [9]. 27

2.12 Phase space information geometry for SL(2,R). Retrieved from [10]. 31

2.13 Markovian-like chain describing action of hamiltonian on $|K_n\rangle$, and the unfolding of the markovian-like chain in a time series, respectively shown with the bottom most nodes representing $|K_n\rangle$. Retrieved from [11]. 34

2.14 Spread complexity of TFD state in the SYK. Retrieved from [11]. 36

3.1 Behaviour of the lanczos coefficients of operator O located at the Z_3 site within an integrable and chaotic time limit. Retrieved from [12]. 42

3.2 Behaviour of arnoldi coefficients of operator O located at the Z_3 site within integrable and chaotic time limits. Retrieved from [12]. 43
3.3 Behaviour of $h_{n,n}$ coefficients of operator O located at the Z_3 site within integrable and chaotic time limits. [12] 44
3.4 Behaviour of off-diagonal coefficients of operator O located at the Z_3 site within integrable and chaotic time limits. Retrieved from [12]. 44
3.5 Behaviour of diagonal d_{nn} coefficients for the non-hermitian terms for both (a) the SYK and (b) 1d lattice model. Retrieved from [13]. 46
3.6 (a,b) eigen-energies for $\gamma = 0.007 < \gamma_c$ and $\gamma = 0.04 > \gamma_c$ respectively. (c) wave functions of 2 modes below gap and (d) behavior of γ_c with n_s. Retrieved from [13]. 47
3.7 krylov complexity in open systems (red) compared to that seen in closed systems. Retrieved from [13]. 48
3.8 complexity of purification for a harmonic oscillator in an open system with different damping values Γ. Retrieved from [14]. 54
3.9 complexity of purification for an inverted oscillator in an open system with different damping values Γ. Retrieved from [14]. 55
3.10 complexity of purification for an inverted oscillator in an open system with different damping values Γ. Retrieved from [14]. 57
3.11 Averaged Spectral form factor for both the gaussian potential (blue) and non gaussian potential with varied parameters g/h. 59
3.12 Averaged gaussian spectral form factor affected by the environment. 60
3.13 Averaged non-gaussian spectral form factor influenced by the environment. 60
3.14 Growth of complexity of gaussian and non-gaussian RMT model through time. . . . 62
3.15 Growth of complexity for open gaussian model. 63
3.16 Growth of complexity of open gaussian and non-gaussian model through time. . . . 63

A STUDY ON COMPLEXITY

Dimakatso Reneilwe Rapotu

Dr. Haque, Thesis Supervisor

Prof. Murugan, Co-supervisor

ABSTRACT

This thesis explores quantum complexity for various quantum systems. Quantum complexity is a well defined quantity in quantum information theory that measures the difficulty of constructing a quantum state from a given reference state and so far various methods within high energy physics communities have been proposed for computing complexity. In this thesis, we will first review the computations of the different methods used for computing complexity, such as the circuit complexity that uses the wave function, Fubini-Study complexity, and finally the recently proposed Krylov complexity for closed quantum systems.

We then extend our investigation and review the complexity for some open quantum systems that have already been explored in literature and finally, we will make some progress by also extending the investigation towards computing the complexity of a new open quantum system, namely the non-gaussian random matrix model.

Chapter 1

INTRODUCTION

1.1 Background and Motivation

Complexity is a topic that has its roots in quantum information theory with its establishment being seen in quantum computers, it is a study that involves knowing how arduous it is in performing an operation. In quantum physics, this has been used as a tool in understanding the building blocks of the theory of particle physics. Within high energy physics, there have been many proposals as to how it should be defined, from an operator approach namely circuit complexity to geometric path integral optimization methods such as the fubini study metric and krylov complexity.

The beginning instances where the term complexity was defined within a quantum field theory is seen in the holographic duality (AdS/CFT) description more particularly in black hole physics [15, 16, 17]. Entanglement entropy (EE) defined on the boundary CFT has its dual description known as the bulk geometry in AdS, with the Bekenstein-Hawking formula (black hole entropy) being its analogous version when applied in black hole physics; and so still keeping within black hole physics, as the black hole thermalizes, the entanglement entropy reaches what is known as saturation while the Einstein-Rosen bridge continually grows.

The quantity that continues to grow on the boundary CFT after thermalisation has been coined as complexity by Susskind et al.[4] and has brought forth with it two definition proposals namely complexity = volume and complexity = action, while these will be better explained in the coming chapter, these bulk theories try best at explaining the physics past the event horizon but lack the precision in giving a set dual definition of complexity within a quantum field theory.

Circuit complexity, krylov complexity and fubini-study metric include some of the methods that have been used in understanding complexity within quantum field theories, the aim of the thesis subsequently includes a study that covers the various quantum systems that have in part been used in understanding complexity, the study extends the methods used in closed systems to open quantum systems to also better characterize the effects that interactions may have on the complexity of a system.

1.2 Thesis Outline

In Chapter 2, we introduce the notion of complexity, the basic definitions and concepts that underpin it, and the ideas that enable the description of complexity in Quantum Field Theory. The different categories that have been brought about to form quatum complexity such as circuit complexity and krylov complexity will also be explored within different systems.

In Chapter 3, we introduce the theory of open quantum systems. This will begin with an introduction that gives a primer on the definition of open quantum systems, followed by an exploration of recent work that has been done in understanding complexity within such a framework. In addition to the exposition of the current work, the thesis will introduce a study on the effects that noise has on the spectral form factor and fidelity of both the gaussian and non-gaussian model random matrix theories, the connection between the krylov complexity and the spectral form factor through the survival amplitude will in also be explored in order to characterize the complexity of the open system.

In Chapter 4, we conclude the thesis and go on to discuss potential directions for future work on the topic of complexity.

Chapter 2

QUANTUM COMPLEXITY

2.1 Complexity

Quantum complexity is a well established concept that is used in quantum information theory, complexity enables the classification between hard operations and easy operations thus allowing one to know how arduous it is in implementing a certain task [18]. The classical analogue of complexity is ubiquitous in computer science and underpins most concepts in computer science such as communication complexity and separation of complexity classes [19]. In physics, complexity arises from the Anti-de Sitter Space/Conformal field theory (AdS/CFT) and has been suggested in examples such as the conjectured correspondence of complexity connected to the properties of black holes within regions beyond the event horizon as will be discussed [18].

Beginning with a quantum circuit model as illustrated in Figure 2.1, the traditional definition of computational complexity starts with some reference state and a unitary operator U that is built with a set of simple gates, complexity thus entails knowing the minimum number of the local gates needed to implement a global unitary operator or a state. While every unitary U can be decomposed into two local unitaries as per figure 2.1, the decomposition is not unique as there are various decompositions, however there is a unique minimal number of gates that are needed to carry out the unitary to get to the target state,

$$|\psi_{target}\rangle = U|\psi_{ref}\rangle$$

the unique number is what is known as the optimal circuit complexity [5, 20]. In the condense matter community, this is an idea that has also been examined by various authors with the term circuit

depth for spin chain states being used [21].

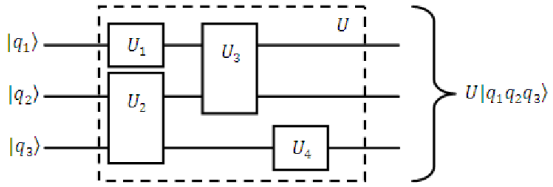

Figure 2.1: Quantum circuit model example. Retrieved from [1].

Working with sequential discrete gates calls for implementing a tolerance threshold that ensures that even if a target state is not reached, a state close to the target state can still be attained -

$$T : ||\psi\rangle - |\psi_{target}\rangle|^2 \leq \epsilon$$

Particular reference states, unitary gates and tolerance threshold have been seen to affect the minimum number of gates resulting in questions as to whether the task is Polynomial in the size of the reference state or Exponential in the size of the reference state; To answer this - the Solovay–Kitaev theorem in quantum computing in part ensures that there exists efficient quantum gates in a system of N-qubits, such that the quantum complexity of the state typically goes exponential in the number of qubits with a dependence on the tolerance parameter: $O(e^N \log(1/\epsilon))$ [22].

Complexity is particularly interesting in chaotic systems, the general features that come from quantum computational complexity in any generalized chaotic system include the evolution behaviour of a quantum operator/state o. The quantum operator o evolves in time in a unitary fashion with the unitary $U = e^{-iHt}$ being described as a set of gates available in the quantum computer [2] :

$$o(t) = e^{iHt} o e^{-iHt}$$

There is a bound on the complexity that goes exponential in the number of degrees of freedom known as the maximal complexity e^N, followed by a period of linear growth before reaching saturation at time scale $t \sim O(e^N)$. At early time the initial growth of complexity starts off non-linearly with an exponential growth lasting for times of order $\log(N)$ with the complexity at the end of this period being of order N, and finally at very large times of $t \sim O(e^{e^N})$ a poincare recurrence is expected as illustrated in Figure 2.2.

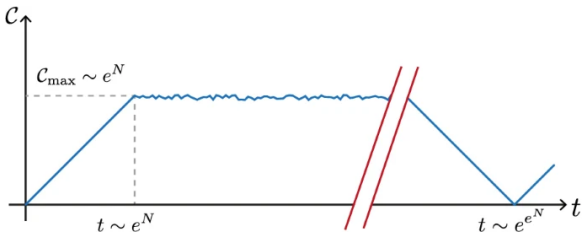

Figure 2.2: Generalized features of computational complexity for a chaotic Hamiltonian. Retrieved from [2].

2.2 Complexity in Holography

With the definition and generalized features of quantum computational complexity in hand, we further explore the term complexity in holography and see how it is better explained using quantum computational methods.

Holography, also known as the AdS/CFT correspondence is a duality between the theory of gravity in the asymptotic Anti-de Sitter space and a quantum theory namely Conformal Field Theory [23, 24] as noted in figure 2.3. The conformal theory is one that exists within d dimension while the AdS exists within dimensions $d+1$, with the holographic principle being brought about by the difference in dimensionality.

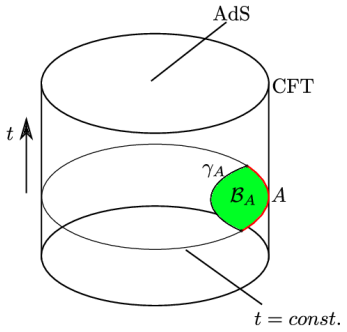

Figure 2.3: AdS/CFT correspondence. Retrieved from [3].

The AdS/CFT enabled the relation between the holographic derivation of entanglement entropy in quantum (conformal) field theories to the minimal area surfaces in asymptotically anti-de Sitter (AdS) spaces and is known as the RT prescription named after Shinsei Ryu and Tadashi Takayanagi [25]. Given a total system that is comprised of sub-system A and B, entanglement entropy informs

one of how strongly entangled a wave function is,

$$\begin{aligned} S_A &= -\mathrm{tr}_A \rho_A \log \rho_A \\ &= -\mathrm{tr}_A \mathrm{tr}_B |\Psi\rangle\langle\Psi| \log \mathrm{tr}_B |\Psi\rangle\langle\Psi| \\ &= \sum \lambda_i \log \lambda_i \end{aligned}$$

Entanglement entropy - EE, gives the entropy that is accessible to system A without receiving any communication from system B. Defining the entanglement entropy S_A of system A on a CFT $\mathbb{R}^{1,d}$ has a proposed related 'Area law' equivalent on AdS_{d+2} -

$$S(A) = \frac{\text{Area of}\gamma_A}{4G_N}$$

and as such holographic entanglement entropy involves investigating the bipartite entanglement on the boundary CFT which, becomes translated into a gravitational problem with a collection of surfaces that extend into the bulk of the AdS, these are observed and subsequently evaluated through using the Bekenstein-Hawking Formula to give what is known as the black hole entropy referenced by equation (2.1) [25].

$$S(A) = \frac{\text{Area of}\gamma_A}{4G_N} \tag{2.1}$$

$$S(A) = \min_{\partial V \sim \sum \frac{A_V}{4G_N}} \tag{2.2}$$

Varying over all possible surfaces to find the minimum, the minimum value for the Bekenstein-Hawking entropy gives the entanglement entropy in the Conformal Field Theory, this has thus brought forth conversations for the bulk-boundary description between quantum information theorists and high energy theorists together [26].

[4] probed the interior of blackholes as in shown Figure 2.4 thus illustrating a black hole in AdS which was conformally transformed and compressed in spacetime. In the figure, the spatial direction run horizontally across the image while time runs upwards, the vertical lines are the asymptotic AdS boundary with the null rays moving at angles of 45°. The cross diagonals are known as the Horizon dividing the rest of the asymptotic infinity from the blackhole.

From the boundary theory view point, Susskind was interested in discussing the singularity region

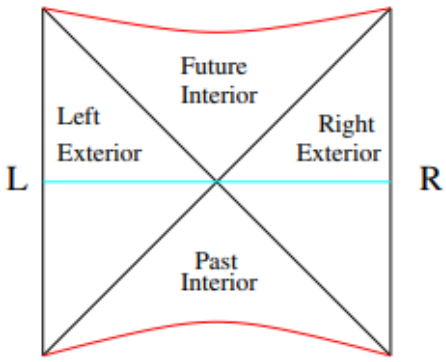

Figure 2.4: Penrose diagram of schwarzchild geometry. Retrieved from [4]

deep in the interior of the black hole as depicted by the geometry of figure 2.4 and as such, the concept of gravity in the conformal field theory was put forth as a Thermofield double state involving two copies of the conformal field theory degrees of freedom brought about by the two boundaries stuck together in a pure state [27] -

$$|\text{TFD}\rangle \simeq \sum_i e^{-\beta E_i/2}|E_i\rangle_L|E_i\rangle_R$$

As both copies move forward with time, this introduces a time dependence -

$$|\text{TFD}\rangle \simeq \sum_i e^{-\beta E_i/2}e^{-iE_i(t_L+t_R)}|E_i\rangle_L|E_i\rangle_R$$

such that a time dependence on the entanglement entropy is seen as -

$$\begin{aligned} S_R &= -\text{tr}_R \rho_R \log \rho_R \\ \rho_R &= \text{Tr}_L |\text{TFD}\rangle\langle\text{TFD}| \\ \rho_R &\simeq e^{-E_{i/T}}|E_i\rangle_R|E_i\rangle_R. \end{aligned}$$

In the geometric framework this leads to the entanglement entropy between the two boundaries as given by the Bekenstein-Hawking formula of the horizon. The holographic entanglement entropy proved to be a great probe of the asymptotic AdS spacetime, however it has been argued that the probe is a poor one in describing the geometry inside the horizon as it only probes the eigenvalues of the density matrix and as such, a new probe that is sensitive to phases was needed.

The new probe would be termed Holographic complexity, in particular Susskind drew attention to probes that related to the asymptopic AdS spacetime. One proposal known as 'Complexity = Volume' [28] has a construction similar to holographic entanglement entropy whereby one chooses a time slice in the boundary theory as seen in figure 2.5(L) where the state of interest would exist, the family of cauchy surfaces that connect the boundaries are varied such that the Volume of the time slices are maximised and consequently associated as the complexity of the particular boundary state namely $C_V(\sum) = \max_{\sum=\partial B}[\frac{V(B)}{G_N l}]$.

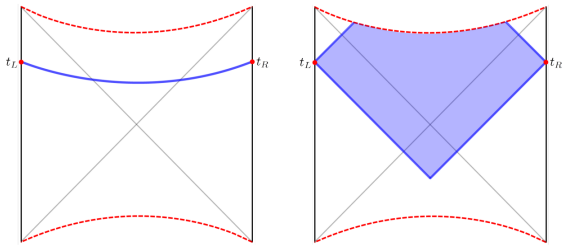

Figure 2.5: Complexity = volume for eternal AdS black hole (left) and complexity = action (right). Retrieved from [5].

Another proposal, complexity = action [29] focuses on the domain of dependence by taking time slices of the boundary while also including null sheets to define a region known as the Wheeler-de-Witt (WDW) patch as depicted by the shaded area of right-sided image of figure 2.5, the gravitational action is evaluated on the particular spacetime which is then associated as the complexity $C_A(\sum) = \frac{I_{WDW}}{\pi\hbar}$. One feature that both of these new gravitational observables have is that they probe deep inside the interior of the black hole for arbitrarily late times implying that, irrespective of how far upwards within the diagram the t_L and t_R are moved, an observable that probes the interior of the black hole will exist.

An additional proposal, complexity = action 2.0 [30] was put forward, which suggests the possibility of taking the WDW patch and, rather than evaluating the action, the spacetime volume becomes evaluated to give results that have similar properties to the previously mentioned complexity = action $C'_V(\sum) = \frac{V_{WDW}}{G_N l^2}$.

While all these are interesting geometric observables, one is led to probe on why these aforementioned complexities are associated with the complexity of the boundary state? One suggestion put forth includes an association found when using the complexity = volume framework whereby, in using the discrete language borrowed from quantum information theory, one can describe the ground

state wave function of critical systems using MERA (Multi-scale Entanglement Renormalization Ansatz) [31]; MERA is known to provide efficient tensor network representation and is seen as a quantum circuit that takes an untangled state of qubits to produce a ground state that is of interest.

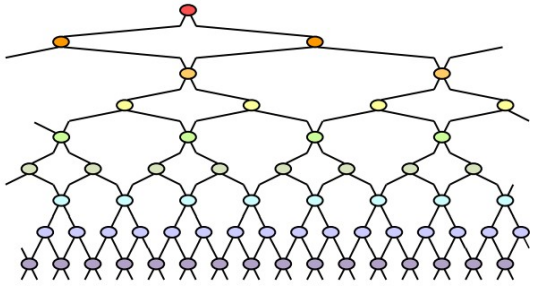

Figure 2.6: Multi-scale entanglement renormalization ansatz. Retrieved from [6].

The geometry from MERA is much like the geometry of the time slice of the AdS [32], therefore knowing the number of gates (illustrated in figure 2.6) is equivalent to evaluating the geometric volume in the AdS; this then draws a natural connection between the volume of cauchy time slices and the holographic complexity framework.

Another reason as to why a connection between the geometric observations and the complexity of the boundary exist is seen with the rate of growth of complexity as the time slices t_L and t_R are pushed towards the singularity. The rate of growth of complexity is known to be proportional to the mass of the black hole, this claim is supported by the features of the Conformal Field Theory - one feature being that there is a large number of degrees of freedom and that the Hamiltonian is chaotic with the spectrum at high energies being more or less random resulting in a linear growth of complexity for long times [29].

The growth is expected to be proportional to the number of degrees of freedom in the conformal field theory while the number of degrees of freedom can be formulated in terms of the entropy. Eventually it is expected that at very late times the complexity saturates, giving rise to notable behaviour as referenced in figure 2.2. The third reason why the aforementioned complexities can be associated with the complexity of the boundary state includes the use of the switch back effect of the Thermofield Double state (TFDS) used in a strongly coupled quantum system [33]; it is seen to be dual to the switchback effect of the C_A complexity where a black hole is probed with perturbations

in order to analyze its reaction.

To re-emphasize, [4] was interested in the features of spacetime deep in the interior and as such brought forth new observables namely; C_A and C_V. There are still however questions about whether these proposals being evaluated are in actual fact the complexity of the boundary state. If the situation is compared to that in holographic entanglement entropy [34], the key difference lies in that entanglement entropy is a quantity that has well established tools and methodologies and results understood.

The problem with the C_A and C_V proposals results from the lack of concrete tools that translate observables in the bulk to those in the CFT, this further leads to the main question; - what will the quantity of complexity really mean in the boundary CFT specifically or in the context of quantum field theory.

2.3 Complexity in QFT

Proposals concerning complexity in Quantum Field Theory (QFT) have been put forward and has included the complexity of states or how hard it is in preparing a particular quantum state which includes the geometric approach proposed by Nielsen [20]

Defining and better understanding complexity in QFT starts with using the most simplest quantum field theory in d dimensions namely the free scalar field theory given by the Hamiltonian below -

$$H = \frac{1}{2}\int d^{d-1}x \left[\pi(x)^2 + \nabla\phi(x)^2 + m^2\phi(x)^2\right].$$

One of the features that [5] noted from the geometry of the theory were its UV divergent quantities caused by the entanglement introduced at short distance scales, therefore in order to regulate the theory it needed to be on a lattice,

$$H = \frac{1}{2}\int d^{d-1}x \left[\pi(x)^2 + \nabla\phi(x)^2 + m^2\phi(x)^2\right]$$
$$H = \frac{1}{2}\sum_{\vec{n}}\left[\frac{\pi(\vec{n})^2}{\delta^{d-1}} + \delta^{d-1}(\frac{1}{\delta^2}\sum_i \left[\phi(\vec{n}) - \phi(\vec{n}-x_i)\right]^2 + m^2)\phi(\vec{n})^2\right]$$

another feature noted was that noted were the degrees of freedom in the theory, leading the discussion to being framed from the perspective of quantum mechanics with the field now being represented by an infinite family of coupled harmonic oscillators -

$$H = \frac{1}{2}\int d^{d-1}x \left[\pi(x)^2 + \nabla\phi(x)^2 + m^2\phi(x)^2\right]$$
$$H = \frac{1}{2}\sum_{\vec{n}}\left[\frac{p(\vec{n})^2}{M} + M\left(\Omega^2\sum_i [x(\vec{n}) - x(\vec{n}-\omega_i)]^2 + w^2\right)x(\vec{n})^2\right]$$

To further simplify the problem at hand [5] further reduced the problem into a two coupled harmonic oscillator -

$$H = \frac{1}{2}\left[p_1^2 + p_2^2 + w^2(x_1^2 + x_2^2) + \Omega^2(x_1 - x_2)^2\right]$$

Using the normal modes of the system reduces it to a problem of uncoupled, two independent single harmonic oscillators -

$$H = \frac{1}{2}\left[p_+^2 + w_+^2 x_+^2 + p_-^2 + w_-^2 x_-^2)+\right]$$

with

$$x_{\pm} = \frac{1}{\sqrt{2}}\left(x_1 \underset{-}{+} x_2\right)$$
$$w_+ = w$$
$$w_- = w^2 + 2\Omega^2$$

and so solving for the wave function for the problem at hand gives the ground state written out as a gaussian -

$$\Psi_0(x_+, x_-) = \Psi_0(x_+)\Psi_0(x_-) \tag{2.3}$$
$$= \frac{(w_+ w_+)^{1/4}}{\sqrt{\pi}}\exp\left[-\frac{1}{2}(w_+ x_+^2 + w_- x_-^2)\right] \tag{2.4}$$
$$\Psi_0(x_1, x_2) = \frac{(w_1^2 - \beta^2)^{1/4}}{\sqrt{\pi}}\exp\left[-\frac{1}{2}w_1 x_1^2 - \frac{1}{2}w_2 x_2^2 - \beta x_1 x_2\right] \tag{2.5}$$
with (2.6)
$$\beta = \frac{w_+ - w_-}{2} < 0 \tag{2.7}$$

2.3.1 Circuit complexity

When applying computational complexity (circuit) to QFT - there are a number of things that need to be specified such as the reference state ψ_r, together with the need of putting each one of the degrees of freedom at each lattice site into a Gaussian state [5] -

$$\psi_r \simeq \exp\left[-\frac{1}{2}w_0^2 \sum x_i^2\right]$$

each site then becomes a separate Gaussian with no entanglement between each of the degrees of freedom and each one of the gaussian states has a translationally invariant coefficient w_0. Next of the things that needs to be specified includes the gates or unitaries used to build the circuit. In the context of quantum mechanics, the natural operators that are typically used are known to be the position and momentum operators but [5] saw it simple to build unitaries Q_{ij} by simply taking exponentials of these operator $x_i p_j$ as shown below whereby, shifting x_j by some factor ϵx_i is seen as entangling between the two degrees of freedom.

$$Q_{ij} = \exp\left[i\epsilon x_i p_j\right] (i \neq j)$$

and scaling x_i to $e^{\epsilon}x_i$ would entail -

$$Q_{ii} = \exp\left[i\epsilon/2(x_i p_i + p_i x_i)\right]$$

The next step entails knowing the type of target state that would be used; while there are a number to be chosen from the first one that [5] looked at was the gaussian ground state as referenced by $\Psi_0(x_1, x_2)$ in equation 2.5, another target state that was of interest was the thermofield double state used by [35] noting that the black hole was dual to it in the CFT. The key feature of both of these states is that they are gaussian meaning that the aforementioned gates should suffice in implementing a transformation form a particular reference state to the desired target state.

A circuit can be built from the many gates that are applied to the reference state in order to get to the desired target state as shown in the example below -

$$\psi_T(x_i) = \ldots \underbrace{Q_{22}^{\alpha_3}}_{\text{Scale } (x_2)} \underbrace{Q_{21}^{\alpha_2}}_{\text{Entangle } (x_1 \text{ and } x_2)} \underbrace{Q_{11}^{\alpha_1}}_{\text{Scale } (x_1)} \psi_R(x_i).$$

Summing up all gates within the circuit will then give the circuit depth, such that for the simplified quantum field theory problem (that has already been mentioned in the beginning of this chapter), the depth is given as -

$$\begin{aligned} D_1 &= \sum |Q_{ij,n}| \\ &= \frac{1}{2\epsilon} \log \left[\frac{w_1^2 - \beta^2}{w_0^2} \right] + \frac{|\beta|}{\epsilon} \sqrt{\frac{w_0}{w_1}} (w_1^2 - \beta^2)^{-1/2} \end{aligned}$$

The value does not characterize complexity nor the minimum number of gates for the problem and so to find the optimal circuit that gives the complexity follows an approach from quantum information literature advocated by [36] using Hamiltonian control theory. The process involves considering all the possible ways of getting from the reference state to the target state with a unitary that is constructed through a number of transformations.

$$\psi_T(x_i) = U_{TR} \psi_R(x_i)$$

The transformations are carried out through discrete steps as one moves through the space of states, the sequences over time materialize as a smooth continuous path, and as suggested by [36] it is often easier to work with smooth functions within a smooth space rather than discrete gates and so unitaries have been better described with the following construction of path ordered exponentials -

$$U_{TR}(s) = \mathcal{P} \exp \left[\int_0^1 ds Y^I(s) O_I \right]$$

The path ordered exponential is then seen as a continuous version of the string of unitary gates. [5] looked at a smooth path through the space of states and introduced a parameter s for the positioning along the path. In the above integral, at each one of the points along the path a gate is implemented or a particular generator is applied as described below

$$O_I = O_{ij} = \frac{i}{2}(x_i p_j + p_j x_i)$$

$Y^I(s)$ are the coefficients that vary along the path informing us which of the generators are used and how hard they are being applied at each one of the points along the path, they can also be viewed as a velocity or a tangent vector along the path,

$$Y^I(s) = \mathrm{Tr}[\partial_s U(s) U^{-1}(s) O_I]$$

and rather than building the final unitary one can think of integrating from zero to one to then characterize the trajectory by applying the $U(s)$ to our reference state, this characterizes each one of the individual states along the path which then sets up the general frame work on circuits and how they are built which, is akin to finding geodesics. A follow up question is then posed as to how one acquires a minimized cost function to the circuit depth D as to get the most optimal circuit.

$$D = \int_0^1 ds \sum_I |Y^I(s)|$$

One of the most natural way to assign the cost function is typically through the use of Finsler geometry or as used by [5], a Riemannian geometry such that the circuit depth consequently becomes defined as such -

$$D = \int_0^1 ds \sqrt{\sum_{IJ} \delta_{IJ} Y^I(s) Y^J(s)} \tag{2.8}$$

The unitary $U(s)$ becomes a geodesic in a riemannian geometry, and so finding the extremal path involves taking the action Y^I and extremizing it through treating it like a lagrangian to solve the equations of motion. Rather than using operators, [5] introduced the use of matrices A_{ij}, with the idea being that the initial state and the final state of the simplified QFT are considered within a space of positive quadratic forms.

$$\psi_r \simeq \exp\left[-\frac{1}{2} x_i A_{ij} x_j\right] \qquad \longrightarrow \qquad A_R = \begin{bmatrix} w_0 & 0 \\ 0 & w_0 \end{bmatrix}$$

$$\psi_t \simeq \exp\left[-\frac{1}{2} x_i A_{ij} x_j\right] \qquad \longrightarrow \qquad A_T = \begin{bmatrix} w_1 & \beta \\ \beta & w_1 \end{bmatrix}$$

The gates are also translated to matrices M_{ij}, consequently simplifying and informing one of the underlying symmetry

$$Q_{ij} = \exp\left[\epsilon O_{ij}\right] \qquad \longrightarrow \qquad Q_{ij} = \exp\left[\epsilon M_{ij}\right]$$

$$O_{ij} = i x_i p_j + \frac{1}{2}\delta_{ij} \qquad \longrightarrow \qquad [M_{ij}]_{ab} = \delta_{ia}\delta_{jb}$$

For the example of the two dimensional harmonic oscillator at hand (the simplified QFT), the symmetry group $GL(2,R)$ gives generators $[M_{ij}]_{ab} = \delta_{ia}\delta_{jb}$ that are then used to find the matrix form of $Y^I(s)$

$$Y^I(s) = \mathrm{Tr}[\partial_s U(s) U^{-1}(s) O_I] \qquad \longrightarrow \qquad Y^I(s) = \mathrm{Tr}[\partial_s U(s) U^{-1}(s) M_I]$$

which is equivalent to finding the geodesic for some right invariant metric on $GL(2,R)$ -

$$ds^2 = \delta_{IJ}\mathrm{Tr}[dU(s)U^{-1}(s)M_I]\mathrm{Tr}[dU(s)U^{-1}(s)M_J]$$

The equation above is then simplified to give the metric -

$$ds^2 = 2dy^2 + 2d\rho^2 + 2\cosh(2\rho)\cosh^2\rho d\tau^2 + 2\cosh(2\rho)\sinh^2\rho d\theta^2 - 8\sinh^2\rho\cosh^2\rho d\theta d\tau \tag{2.9}$$

with (y, ρ, τ, θ) giving co-ordinates that parameterizes the trajectory or circuits $U(s)$ in $GL(2,R)$ -

$$U(s) = e^{y(s)} \begin{bmatrix} \cos\tau(s)\cosh\rho(s) - \sin\theta(s)\sinh\rho(s) & -\sin\tau(s)\cosh\rho(s) + \cos\theta(s)\sinh\rho(s) \\ \sin\tau(s)\cosh\rho(s) + \cos\theta(s)\sinh\rho(s) & \cos\tau(s)\cosh\rho(s) + \sin\theta(s)\sinh\rho(s) \end{bmatrix}$$

which are the geodesics connecting $U(s=0)$ to $U(s=1)$ with the target state A_T

$$A_T = \begin{bmatrix} w_1 & |\beta| \\ |\beta| & w_1 \end{bmatrix} = w_0 U(1) U^T(1)$$

whereby $U(1)U^T(1)$ is defined as follows -

$$U(1)U^T(1) = e^{2y_1} \begin{bmatrix} \cosh 2\rho_1 - \sin(\theta_1+\tau_1)\sinh 2\rho_1 & \cos(\theta_1+\tau_1)\sinh 2\rho_1 \\ \cos(\theta_1+\tau_1)\sinh 2\rho_1 & \cosh 2\rho_1 + \sin(\theta_1+\tau_1)\sinh 2\rho_1 \end{bmatrix}$$

The boundary conditions given the above constraints of the geodesic, are then found to be:

$$\begin{aligned} y_1 &= \frac{1}{2}\log\frac{w_1^2 - \beta^2}{w_0^2} = \frac{1}{2}\log\frac{w_+ w_-}{w_0^2} \\ \rho_1 &= \frac{1}{2}\log\frac{w_1 + |\beta|}{w_1 - |\beta|} = \frac{1}{2}\log\frac{w_-}{w_+} \\ \theta_1 + \tau_1 &= \pi \end{aligned}$$

Solving for the geodesics, the shortest geodesic is found (as illustrated in green in figure 2.7 below) and so even in the complicated geometry, the minimal geodesic with the corresponding circuit $U(s)$ is given by

$$\tau(s) = 0 \qquad \theta(s) = \pi$$
$$y(s) = y_1(s) \qquad \rho(s) = \rho_1(s)$$

$$U(s) = Pe^{\int_0^s \begin{bmatrix} y_1 & -\rho \\ -\rho & y_1 \end{bmatrix}} \longrightarrow U(s) = \mathcal{P}\exp\left[\frac{1}{2}M_{--}\log\frac{w_-}{w_0}s + \frac{1}{2}M_{++}\log\frac{w_+}{w_0}s\right]$$
$$\text{with} \quad M_{\pm\pm} = \frac{1}{2}(M_{11} + M_{22} + M_{12} + M_{21})$$

The circuit complexity for the two coupled harmonic oscillator is then calculated,

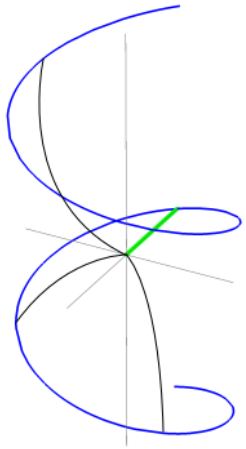

Figure 2.7: pictorial representation of geodesic corresponding to the complexity through circuit complexity metric. Retrieved from [5].

$$C = D_{min} = \sqrt{2\rho_1^2 + 2y_1^2}$$
$$= \sqrt{\log^2\frac{w_+}{2w_0} + \log^2\frac{w_-}{2w_0}}$$

Having learnt from the case above, of the two coupled harmonic ocillators, [5] then examined the lattice of N^{d-1} oscillators with simplified parameters of $\Omega \longrightarrow 0$, the target state for a periodic

square NxNxN... lattice as calculated by [5] becomes

$$\psi_T \simeq \exp\left[-\frac{1}{2\delta}\sum w_{\vec{k}}|x_{\vec{k}}|^2\right]$$

where

$$w_{\vec{k}}^2 = m^2 + \frac{4}{\delta^2}\sum \sin^2\frac{\pi k_i}{N}$$
$$k_i = 0, 1, ..N-1$$

while the target state is simplest to describe using normal modes on the lattice, the reference state $\psi_R(x_i) \simeq \exp\left[-\frac{1}{2}w_0^2\sum|x_{\vec{k}}|^2\right]$ remains a set of decoupled gaussians when expressed in terms of normal modes. Using the riemannian geometry and the F_2 cost function given by equation 2.1, the complexity of the vacuum state takes the value -

$$C_{vac} = \frac{1}{2}\sqrt{\sum \log^2\left[\frac{w_{\vec{k}}}{\delta w_0^2}\right]}$$

Summing over all the nodes leads to a domination of UV nodes $k_i \sim \frac{N}{2}$ to which replacing the frequencies $w_{\vec{k}} \sim \frac{1}{\delta}$ leads the complexity in taking the form -

$$C_{vac} \sim \sqrt{\frac{V}{\delta^{d-1}}}$$

The ratio above was seen in holographic complexity $C_{holo} \sim \frac{V}{\delta^{d-1}}$ with [37] suggesting that the difference between the two ratio's could be as a result of strong CFT coupling with many degrees of freedom witnessed in C_{holo}. [5] showed how the complexity model for a free scalar field demonstrated similarities to the holographic proposals for complexity of boundary CFT edging us closer to better understanding and defining complexity in QFT, while the outlook regarding complexity has been vast [38, 7] also demonstrated an alternative method through the Fubini-Study metric to calculate complexity as will be discussed.

2.3.2 Fubini-Study complexity

Complexity through the Fubini-study metric as detailed by [7] involved the study of the ground state of the hamiltonian H_1 of a free bosonic field theory under a quench protocol -

$$H_1 = \sum_{k=0}^{N-1} w_{1,k} \left[(\mathcal{U}_k^2 + \mathcal{V}_k^2)\tau_k^2 + (\mathcal{U}_k\mathcal{V}_k)\tau_k^+ + (\mathcal{U}_k\mathcal{V}_k)\tau_k^- \right]$$

with

$$\mathcal{U}_k = \frac{w_{1,k} + w_k}{2\sqrt{w_{1,k}w_k}}$$
$$\mathcal{V}_k = \frac{w_{1,k} + w_k}{2\sqrt{w_{1,k}w_k}}$$

Fubini-study complexity also includes the use of a reference state $|\psi_0\rangle = \prod_{k=0}^{N-1} |k, -k\rangle$ and a target state which in [7] was the time-evolved state $|\psi_1(t)\rangle = U_1(t)|\psi_0(t=0)\rangle$ that was also decomposed as per [39] -

$$|\psi_1(t)\rangle = \prod_{k=0}^{N-1} N_k(t) \exp(\gamma_{1,k}^+(t) a_k^\dagger a_{-k}^\dagger)|k, -k\rangle \tag{2.10}$$

whereby

$$\gamma_{1,k}^+ = \frac{\alpha_{1,k}^+}{\mu_{1,k}} \left(\frac{\sinh(\mu_{1,k})}{\cosh(\mu_{1,k}) - \frac{\beta_{1,k}}{2\mu_{1,k}} \sinh(\mu_{1,k})} \right)$$
$$\mu_{1,k}^2 = \frac{\beta_{1,k}^2}{4} - \alpha_{1,k}^+ \alpha_{1,k}^-$$
$$\beta_{1,k}^2 = -itw_{1,k}(\mathcal{U}_k^2 + \mathcal{V}_k^2)$$
$$\alpha_{1,k}^- = \alpha_{1,k}^+ = -itw_{1,k}(\mathcal{U}_k\mathcal{V}_k)$$

The target state can be viewed as a SU(1,1) coherent state with the state manifold being given as a riemannian structure together with the class of states being given as -

$$|\psi\{\gamma_{k,\tau}(t)\}\rangle = \prod_{k=0}^{N-1} N_k(t) \exp(\gamma_{1,k}^+(t) a_k^\dagger a_{-k}^\dagger)|k, -k\rangle$$

Taking the Fubini-study line element in terms of τ

$$\left(\frac{ds}{d\tau}\right)^2 = \left\langle \frac{d\psi}{d\tau} \middle| \frac{d\psi}{d\tau} \right\rangle - \left\langle \frac{d\psi}{d\tau} \middle| \psi \right\rangle \left\langle \psi \middle| \frac{d\psi}{d\tau} \right\rangle$$

gives the metric -

$$ds^2 = \sum_{k=0}^{N-1} \frac{|d\gamma_{k,\tau}|^2}{1 - |\gamma_{k,\tau}|^2}$$

with

$$\gamma_{k,\tau} = \tanh\left(\frac{\phi_k}{2}\right) \exp(i\phi_k)$$

$$ds^2 = \frac{1}{4} \sum_{k=0}^{N-1} (d\theta_k^2 + \sinh(\theta_k)^2 d\phi_k^2).$$

Complexity from the Fubini-study approach takes into account the geodesic distance C_k between the reference state and target state, and as such takes into account two arbitrary points $(\theta_{1,k}, \phi_{1,k})$ $(\theta_{2,k}, \phi_{2,k})$ and uses the metric to calculate the complexity as by [7] -

$$C_{FS} = \sqrt{\sum_{k=0}^{N-1} C_k^2}$$

$$C_{FS} = \frac{1}{2} \sqrt{\sum_{k=0}^{N-1} (\text{arccosh}[\cosh(\theta_{1,k}) \cosh(\theta_{2,k}) - \sinh(\theta_{1,k}) \sinh(\theta_{2,k}) \cos(\phi_{1,k} - \phi_{2,k})])^2}$$

Taking the reference state $|\psi_0\rangle = \prod_{k=0}^{N-1} |k, -k\rangle$ and target state as referenced by equation 2.10 with respect to the two arbitrary points, then $(\theta_{1,k} = 0)$ and $(\theta_{2,k} = 2\text{arctanh}|\gamma_{1,k}|)$, consequently simplifying the complexity to

$$C_{FS} = \sqrt{\sum_{k=0}^{N-1} (\text{arctanh}|\gamma_{1,k}|)^2}$$

Complexity through the Fubini-study approach takes the ground state of the hamiltonian at hand and identifies it as a coherent state of a set group corresponding to the symmetry of the hamiltonian, the metric is subsequently defined on the group manifold enabling the complexity to be defined as the geodesic distance between the reference state and the target state.

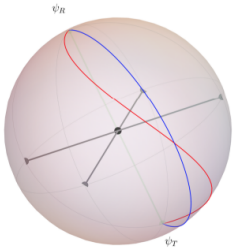

Figure 2.8: Pictorial representation of geodesic (blue) corresponding to the complexity through Fubini-study metric between ψ_R and ψ_T. Retrieved from [7].

2.4 Krylov Complexity

Krylov complexity is another notion of complexity that does not need unitary gates, tolerance parameters, the search for minimum number of gates and as such, there is no essential need for geodesics or metrics meaning that all that is needed to be known to understand the system's complexity is how the operator evolves through time under the unitary operator. The conception of this complexity has also been under-girded by the interest of understanding the quantum phenomenon of long time scale in black hole physics within the Ads/CFT background.

Krylov complexity as proposed by [9] is underpinned by the Krylov subspace; from definition the Krylov subspace named after Russian applied mathematician Alexei Krylov [40], is the smallest subspace of the operator space that has the time evolution of some observable at all times [41]. Krylov complexity within a quantum mechanical framework begins with exploring the complete Hilbert space $\mathcal{H}$ [8], where a quantum operator grows in time in a unitary fashion; this evolves in the Heisenberg framework as depicted by the equation -

$$O(t) = e^{iHt} O e^{-iHt}$$

and so using the Baker-Campbell-Hausdorff decomposition converts the above equation into a Taylor series type decomposition -

$$O(t) = O - it[H, O] + \frac{(it)^2}{2!}[H, [H, O]] + ...$$

showing that the operator evolves in time - it is a linear combination in the subspace spanned by both the operator and the nested commutators that are inclusive of the Hamiltonian and as such, it is noted that as time grows larger the importance of the commutators with Hamiltonians in the growth of the operator also grows [9, 8].

Using the Liouvillian defined as a commutator together with the Hamiltonian -

$$\mathcal{L} := [H, \cdot]$$

we can identify the subspace spanned by the operator and nested commutators of the hamiltonian as the Krylov subspace of the Liouvillian operator -

$$\begin{aligned}\mathcal{H}_O &= \text{Span}\{O, [H, O], [H, [H, O]], ...\} \\ &= \text{Span}\{\mathcal{L}^n O\}_{n=0}^{+\infty}\end{aligned}$$

The dimension of the Krylov subspace is retrieved through the analysis of the finite d dimensional hilbert space and some energy basis $\dim(\mathcal{H}_O) = K$; K is then determined through the rank of $(O, \mathcal{L}O, \mathcal{L}^2O, ..., \mathcal{L}^nO)^T$. The operator is then expanded in the energy basis: $(E_a|E_a\rangle)$ for $\{a = 1, ...d\}$ -

$$O = \sum_{ab=1}^{d} O_{ab}|E_a\rangle\langle E_b|$$

The ket-bra terms are known as the eigenstates of the Liouvillian and also have correspondingly defined eigenvalues of $\omega_{ab} := E_a - E_b$

$$\mathcal{L}|E_a\rangle\langle E_b| = \omega_{ab}|E_a\rangle\langle E_b|$$

The powers of the Liouvillian act on an operator enabling another form of representation in the energy basis of the hamiltonian,

$$\mathcal{L}^n O = \omega_{ab}^n \sum_{ab} O_{ab}|E_a\rangle\langle E_b| \tag{2.11}$$

Solving for the above equation (2.11) gives a Vandermonde matrix whose rank is given by calculating the determinant of the phases $\{\omega_{ab}\}$ in the matrix -

$$\Delta(\{\omega_{ab}\})\Pi_{i,j=1}^{d} O_{ij}$$

The rank of the Vandermonde matrix is at most d^2 due to the matrix having d^2 columns, assuming that a dense operator has non-zero projection in every eigenstate of the Liouvillian and that there are no degeneracies in the spectrum of the Liouvillian, this will give the largest possible Krylov space dimension $K = d^2 - d + 1$ [8].

In chaotic systems, level repulsion (the lack of intersecting energy levels/bands) in the energy spectrum is expected, therefore no degeneracies are expected in the energy spectrum and as such

no degeneracies in the liouvillian spectrum are to be expected. Local operators are usually expected to follow the Eigenstate Thermalization Hypothesis (ETH) [42] suggesting that they are dense in the energy basis, leading to the conclusion that in chaotic systems a saturated bound is expected [8].

In Integrable systems, a general poisson statistic in the energy spectrum is expected such that degeneracies and quasi-degeneracies in the Liouvillian spectrum are also expected; a simple example of integral systems referenced by [8] shows how free systems are much below the bound of the Krylov space $K = d^2 - d + 1$.

Having looked at the hamiltonian of a fermionic harmonic oscillator which satisfies the anti-commutation relations -

$$H = \sum_{i=1}^{N} w_i c_i^\dagger c_i$$

and taking the single fermion operator -

$$O = \sum_{i=1}^{N} o_i c_i + o_i^* c_i^\dagger$$

commutations with the hamiltonian leave the operator in a single fermion sector implying that the Krylov space has dimension $K \leq 2N$. Constructing an orthonormal basis for the Krylov space includes defining the inner product for the operators; the inner product can be the infinite temperature inner product or any arbitrary inner product, the simplest choice for the above example includes taking the trace of the product of the operators [8].

The first step in building a Krylov basis involves normalizing the seed operator, followed by commuting the normalized seed operator with the hamiltonian and removing the projection of the commutator from the normalized seed function. The norm is then defined which, when normalized, gives the next operator and subsequently defines a new operator.

The lanczos algorithm gives a general recurrence equation for the nth operator [43], it allows an input of any arbitrary hermitian operator O and hamiltonian, the first three steps as mentioned above include normalizing the seed operator in order to define the first element.

In an automated manner one proceeds the process for n greater than one, the nth element is then

Lanczos algorithm	
1.	set $b_0 := 0$ and $\|O_{-1}) := 0$
2.	let $\|O_0) = \frac{1}{\sqrt{(O\|O)}}\|O)$
3.	when $n >= 1 \rightarrow \|A_n) = L\|O_{n-1}) - b_{n-1}\|O_{n-2})$
4.	let $b_n = \sqrt{(A_n\|A_n)}$
5.	if $b_n = 0$ break, else set $\|O_n) = \frac{1}{b_n}\|A_n)$ and proceed to step 3.

Table 2.1: Lanczos algorithm

defined as the commutator of the hamiltonian and the previous O_{n-1} operator less the multiplication of the previous lanczos coefficient and the operator O_{n-2}; the norm of the nth element is computed and if its equal to zero the algorithm stops, otherwise the algorithm continues and defines the next operator in the Krylov basis by dividing the nth element with the computed lanczos coefficient.

The algorithm should terminate as once all directions are exhausted in the Krylov subspace, and once all projections (i.e. a gram-schmidt) at every step are removed, there is no new directions to explore thus resulting in a zero operator that has a zero norm. The output of this algorithm gives a basis known as the Krylov basis resulting in the lanczos sequence.

Once this is completed, a basis with orthonormality is retrieved; an important feature of the Krylov basis that should be noted is that, it is ordered according to the number of nested commutators with the hamiltonian while the Liouvillian is tri-diagonal in the Krylov basis. The Krylov basis is then used to expand time-dependant operators with complex time-dependant coefficients to make them hermitian -

$$O(t) = \sum_{n=0}^{K-1} i^n \psi_n(t) O_n.$$

Using the heisenberg time-evolution equation,

$$\frac{d}{dt}O(t) = i[H, O(t)]$$

we find the differential recurrence equation for the $\psi_n(t)$ with only a dependence on the lanczos coefficients and an initial condition -

$$\dot{\psi_n}(t) = b_n\psi_{n-1}(t) - b_{n+1}\psi_{n+1}(t) \tag{2.12}$$

$$\psi_n(0) = \delta_{n0}.$$

Essentially, if one studies the wave functions ψ_n then all the information regarding the evolution of the operator is known. The boundary condition $\psi_n(0) = \delta_{n0}$ ensures that the operator begins at the first krylov element O_0, the dynamics thereafter of the operator along the Krylov basis depends only on the lanczos coefficients b_n, and as mentioned by [9] one could think of the ψ_n's as wave functions in the Krylov basis with the sense that they are the time dependant projection of the operator $O(t)$ on the Krylov basis element O_n. From the unitary we have that the norm of this wave function is one - intrinsically showing how the time evolution of an operator on the Krylov basis is to be analyzed -

$$O(t) = \sum_{n=0}^{\infty} \frac{(it)^n}{O_n}$$

Krylov complexity is then thought of as a probe of the time dependent profile of the wave function $\psi_n(t)$ with the first probe introduced by [9] being the average position on the Krylov chain (it is termed chain as it is ordered) -

$$C_k(t) = \sum_{n=0}^{K-1} n|\psi_n(t)|^2$$

Later [44] introduced another probe of the time dependent profile - the average amount of randomness which is the usual way to define entropy on a distribution, resulting in [9] naming it K-entropy -

$$S_k(t) = \sum_{n=0}^{K-1} |\psi_n(t)|^2 \log|\psi_n(t)|^2$$

There are many ways to probe the wave function $\psi_n(t)$ to describes the time evolution of an operator. Numerical results from [8] of the SYK model with four fermion interaction (known to be a maximally chaotic quantum system as it features level repulsion), has operators that satisfy the Eigenstate Thermalisation Hypothesis and saturate the bound on the lyapunov exponent. Working in a finite number of fermion N system to study long-time effects,[8] investigated the complex syk-4 that involves L-complex fermions -

$$H_{syk} = \sum_{i,j,k,l}^{L} J_{ij;kl}c_i^\dagger c_j^\dagger c_k c_l \tag{2.13}$$

these fermions satisfy anti-commution relations; the hilbert space dimension for L-complex fermions is $2^{L/2}$ while the hermitian hopping operator for the model that was used is given by -

$$O = c^{\dagger}_{L-1}c_L + c^{\dagger}_L c_{L-1} \tag{2.14}$$

In [45] it was shown that the operator obeys the Eigenstate Thermalization Hypothesis and as such [8] worked in a fixed occupation sector of the hamiltonian as both the hamiltonian and operator commute with the number operator; this implies that when one works with both the hamiltonian and operator an occupation sector is not excluded, this then saw [8] working in the biggest sub sector which is a half filled sector. For the complex syk-4 it was expected for the Krylov space to saturate the bound as it satisfies level repulsion and ETH.

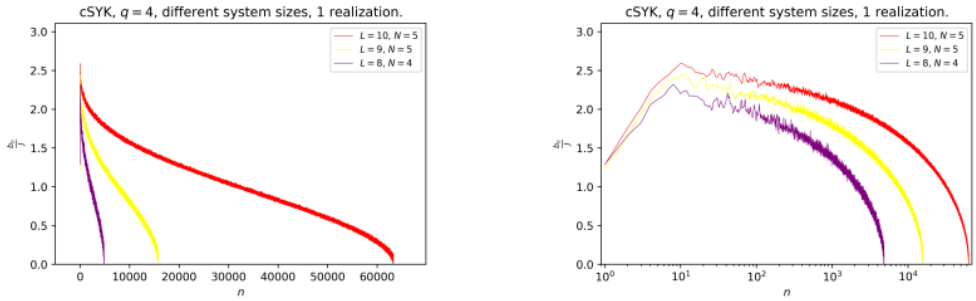

Figure 2.9: Lanczos sequences for L = 8, 9, 10 in linear (left) and logarithmic (right) scale along the horizontal axis. Retrieved from [8].

The various lanczos sequences for the syk with eight, nine and ten fermions is shown respectively in the above figure, the behaviour of the lanczos coefficients tends to zero with a slow descent. [8] further noted a non-perturbative small slope of order $-e^{-2S}$ with S denoting the entropy of the system, the descent of the lanczos coefficients is also believed to be a characteristic of quantum chaotic systems.

K-complexity has features expected from quantum complexity, it was shown that the K-complexity is naturally bounded by the krylov space dimension and that in chaotic systems, saturation occurs at time scales of $O(e^{2L})$ as suggested by the figure 2.10. The calculation of the lanczos coefficients has been noted to computationally challenging [8] and as such the end of the Krylov space suffers numerical instability resulting in the need to go to high precision, however one can use other methods and systems to calculate the lanczos coefficients to better characterise quantum chaotic systems as will be discussed in the following section.

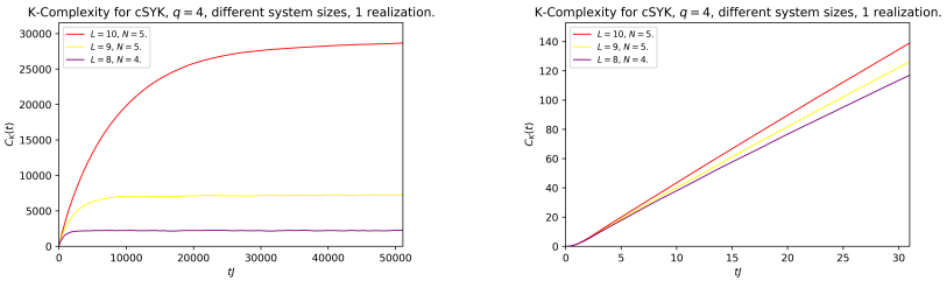

Figure 2.10: Comparison of K-complexity for L = 8, 9, 10 for exponentially long times (left) and for early times (right). Retrieved from [8].

2.4.1 Krylov complexity through the two-point function

A two point function or auto correlation of an operator is given by an inner product of the time evolved operator with itself and has a specific taylor series that gives the moments, it is also thought of as a probability amplitude of doing an evolution while staying in the same state as in the beginning

-

$$C(t) = (O|O(t)) = (O_0|e^{it\mathcal{L}}|O_0) = \sum_{n=0}^{\infty} \frac{t^{2n}}{2n!}\mu_{2n} \tag{2.15}$$

The moments of the auto-correlation $C(t)$ are given by -

$$\mu_{2n} = (O_0|\mathcal{L}^{2n}|O_0) \tag{2.16}$$

and are related to the Dyck paths leading to an invertible relation between the moments and the lanczos coefficients [9]. The strategy for studying the thermodynamic limit includes considering two point functions and the asymptotics of the moments/lanczos coefficients. The moments are also related to the Fourier transform through an integral with $\Phi(\omega)$ being the Fourier transform of $C(t)$

$$\mu_{2n} = \frac{1}{D}\sum_{a,b=1}^{D} \omega_{ab}^{2n}|O_{ab}|^2 = \int_{-\infty}^{+\infty} d\omega \frac{\omega^{2n}}{2\pi}\Phi(\omega) \tag{2.17}$$

[9] formulated the hypothesis in the thermodynamic limit by beginning from a known bound on the tail of the fourier transform of the two-point function; for a q-local hamiltonian and for any q-local operator the fourier transform of the two point function is at most exponentially decaying with some

factor κ governed by the geometry of the problem -

$$\Phi(\omega) < \exp\left(\frac{\kappa\pi|\omega|}{2}\right) \tag{2.18}$$

[9] noted that starting the fourier transform of a two-point function with the spectral profile: $\Phi(\omega) \approx \exp(\frac{\pi|\omega|}{2\alpha})$ implies that along the imaginary axis, the two point function has a singularity - the pole of $C(t)$ at $t = \frac{i\pi}{2\alpha}$. The pole scales inversely with the coefficients α suggesting asymptotics for the moments and resulting in asymptotically linearly growing lanczos coefficients.

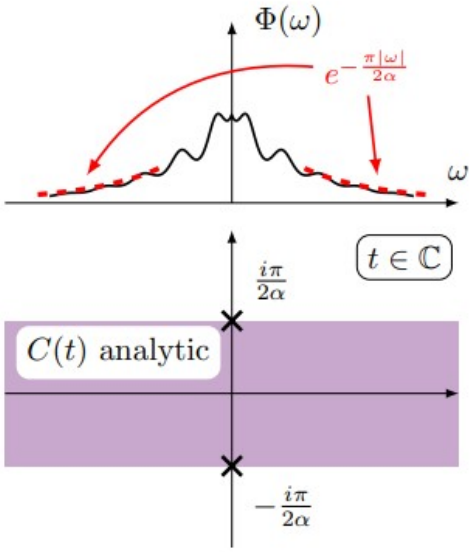

Figure 2.11: Spectral function $\Phi(\omega)$(above) and analytical function of correlation function $C(t)$. Retrieved from [9].

The universal growth hypothesis that [9] proposed shows how in chaotic systems the lanczos coefficients grow fast - which is linear with a slope that is bounded from above by a system dependent geometrical factor; this is the expectation for chaotic systems in the thermodynamic limit and implies exponential growth of complexity. To this end one can see that the pole structure of auto correlation function also provides information about chaos.

2.4.2 Geometry of krylov complexity

Another novel geometric perspective developed by [10] shows how operator growth within Krylov complexity can be approached. A link between the unitary evolution, Liouvillian and the displacement operator demonstrates a mapping of operator growth to the classical motions found in phase space;

the geometry and geodesics represent the operator growth with the volume being proportional to Krylov complexity. Although Krylov complexity can be carried out independent of geodesics, the geometric approach provides an efficient way of decoding the lanczos coefficients given the symmetries that govern the system at hand.

Starting from the definition of the Liouvillian, the Liouvillian operator is known to be tri-diagonal implying the following decomposition when it acts on the vector O_n -

$$\mathcal{L}|O_n) = b_n|O_{n-1}) + b_{n+1}|O_{n+1})$$

it has a matrix representation in the Krylov basis with the elements on the diagonal being zero-valued while the off diagonal elements are known as the lanczos coefficients (b_n's). The geometric approach includes defining the Liouvillian operator in the Krylov basis in terms of ladder operators (L_+, L_-),

$$\mathcal{L} = \alpha(L_+ + L_-) \tag{2.19}$$

such that

$$\alpha(L_+|O_n) = b_{n+1}|O_{n+1})$$

$$\alpha(L_-|O_n) = b_n|O_{n-1})$$

To write the Liouvillian in this way, one needs to know about the symmetry structure of the governing hamiltonian to fully construct the geometric representation of the Liouvillian. This is a commanding representation that sheds light on the constituents of the lanczos coefficients; If the ladder operators are part of some lie algebra then this gives predictive power and an efficient interpretation for the lanczos coefficients without involving much numerical calculations.

Systems that have symmetry generating algebras or spectrum are common for studying the evolution of hamiltonians and are written in terms of algebraic generators; these allow for exactly solvable solutions of certain systems and as such [10] used the intuition in terms of the Liouvillian and Krylov basis. Applying the idea to the SL(2,R) algebra known for representing the SYK and knowing that the groups' three generators satisfy the commutation relation -

$$[L_0, L_\pm] = \mp L_{\pm 1}$$

$$[L_1, L_-] = L_0$$

the Liouvillian represented in the Krylov basis as seen in equation 2.19 is written as the sum of its raising and lowering operators with L_{-1} playing the abstract role of the raising operator L_+, and L_1 playing that of the lowering operator L_- -

$$\mathcal{L} = \alpha(L_{-1} + L_1)$$

The representation for the SL(2,R) generators applied to some highest weighted state gives a simple action in the algebra -

$$\begin{aligned} L_0|h,n\rangle &= (h+n)|h,n\rangle \\ L_{-1}|h,n\rangle &= \sqrt{(n+1)(2h+n)}|h,n+1\rangle \\ L_1|\underbrace{h,n\rangle}_{|O_n)} &= \underbrace{\sqrt{n(2h+n-1)}}_{b_n}|h,n+1\rangle \end{aligned}$$

thus allowing for an association of the Krylov basis $|O_n)$ to the lie algebra and the lanczos coefficients b_n to the value when actioning the lowering operator on the state. Applying the results to the SYK model that is represented by the SL(2,R) group, the dynamics of the operator growth are easily deduced without the need of a numerical approach as it is noted that the Krylov basis and lanczos coefficients are given by the above equations.

The concept of symmetry carries through to another geometric topic, namely that of generalized coherent states. Given that an operator can be given in terms of the Krylov basis and the super operator Liouvillian -

$$|O(t)) = e^{it\mathcal{L}}|O)$$

using the geometric representation of the Liouvillian with our operator $O(t)$

$$|O(t)) = e^{it\alpha(L_{-1}+L_1)}|O)$$

[10] noted that the unitary evolution with the Liouvillian is but the displacement operator $D(\zeta) = e^{\zeta L_{-1} - \bar{\zeta}L_1}$ with the complex parameter $\zeta = \frac{1}{2}\rho e^{i\phi}$; this in turn gives the coherent states for SL(2,R) and SU(1,1) [39] that parameterizes a unit disk - the operator expanded in the Krylov basis then becomes a displacement operator of the generalized symmetry acting on the highest weight state.

Observing the coherent state of SL(2,R) or SU(1,1) given by the form -

$$|z,h\rangle = \sum_{n=0}^{\infty} e^{in\phi} \sqrt{\frac{\Gamma(2h+n)}{n!\Gamma(2h)}} \frac{\tanh^n(\rho/2)}{\cosh^{2h}(\rho/2)} |k,h\rangle$$

and comparing it with the the explicit wave function solution of the Schrodinger equation (equation 2.12) for the SYK:

$$\psi_n(t) = \sqrt{\frac{\Gamma(\eta+n)}{n!\Gamma(2\eta)}} \frac{\tanh^n(\alpha t)}{\cosh^{\eta}(\alpha t)} |k,h\rangle$$

one can note that the growth of the operator from the typical lanczos algorithmic approach is nothing but the coherent state for the particular value of $\rho = 2\alpha t$ and $\phi = \pi/2$ giving a trajectory in phase space - in other words one can think about the operator $O(t)$ in Krylov basis states as a coherent state for a particular value of the complex parameter.

$$|O(t)) = |z = i\tanh(\alpha t), h = \eta/2\rangle$$

The operator growth is a trajectory in phase space and this is possible through representing the Liouvillian by the ladder operators in the Krylov space. The Fubini study metric or known by others as the Information metric is another important concept used in conjunction with coherent states.

$$ds^2_{FS} = \langle dz|dz\rangle - \langle dz|z\rangle\langle z|dz\rangle$$

One can associate the coherent states with the natural Fubini-study metric which for the SL(2,R) becomes a hyperbolic disk metric -

$$ds^2_{FS} = \frac{2hzdz}{(1-z\bar{z})^2} = \frac{h}{2}(d\rho^2 + \sinh^2(\rho)d\phi^2)$$

The operator growth for the SYK model as studied by [10] is a geodesic in a manifold/phase space given by $\rho = 2\alpha t$ and $\phi = \pi/2$, moreover they observed a universal relation between the Krylov complexity and the volume in the metric that is given by -

$$V_t = \int_0^{2\alpha t} d\rho \int_0^{2\pi} d\phi\sqrt{g} = 2\pi h \sinh^2(\alpha t) = \pi K_O$$

and so if one computes the volume in this metric then the Krylov complexity is given as a multiple of π. The geometric interpretation of lanczos coefficients and Krylov complexity holds in all examples such as the heisenberg-weyl and SU(2) algebra studied by [10] with generalized coherent states.

Figure 2.12: Phase space information geometry for SL(2,R). Retrieved from [10].

As illustrated in the shaded yellow region in figure 2.12, the operator growth is seen as a certain trajectory in the Fubini-study metric/hyperbolic disc; for $O(t = 0)$ and starting with some operator when $\rho = 0$, as time progresses the operator goes along the direction $\phi = \pi/2$ and should the operator halt at some time t, this consequently determines the value of $\rho = \alpha t$ enabling the computation of the volume/area encircled by this unit disk which is proportional to $\pi\sqrt{K_O}$.

2.4.3 Growth of states in krylov basis

The Krylov basis as probed in [11] can also be used to capture the growth of states with complexity being termed as a measure of the spread of the wave function across time in the hilbert space, hence the name spread complexity. Starting from a state -

$$|\psi(t)\rangle = e^{-iHt}|\psi(0)\rangle$$

given by some initial vector and a unitary evolution, [11] defined complexity as a spread of this state in the Hilbert space with a choice of some basis in the Hilbert space $B = \{|B_n\rangle : n = 0, 1, 2, ...\}$ such that B_0 is given by the initial state $|\psi(0)\rangle$. [11] argued that one can introduce a cost function or a family of cost functions with which one chooses these basis vectors $|B_n\rangle$, this is then followed by computing the probability that comes from overlapping the state and the basis vectors weighted by

the cost function coefficients c_n.

$$C_B(t) = \sum_n c_n |\langle \psi(t)|B_n\rangle|^2 := c_n p_B(n,t)$$

When the above quantity is minimized over all choices of the basis for some finite amount of time, the minimum - a natural definition to complexity, is then attained through the Krylov basis -

$$C(t) = \underbrace{\min_B c_n C_B(t)}_{\text{krylov basis minimum}}$$

so if the coefficients are monotonic $c_n = n$, and positive in n with any powers, then a state $|\psi(t)\rangle$ can be decomposed into the Krylov basis together with orthogonal factors as -

$$|\psi(t)\rangle = e^{-iHt}|\psi(0)\rangle = \sum_n \phi_n(t)|K_n\rangle \tag{2.20}$$

The idea of the growth/spread of the state in the Krylov basis can then be interpreted as Krylov complexity occurring in the Hilbert space; once the state is expanded in the Krylov basis (equation 2.20), $\phi_n(t)$ gives the probability distribution of how the state is supported on all the orthornormal set of basis vectors in the hilbert space. From the probability distribution, one can then quantify the spread - this growth of the state can be characterized through different quantum information tools such as K-entropy $C_{H_B}(t)$ -

$$\begin{aligned} C_{H_B}(t) &= e^{H_B} \\ &= e^{-\sum_n p_B(n,t)\log p_B(n,t)} \\ &= e^{-\sum_n |\phi_n|^2 \log |\phi_n|^2} \end{aligned}$$

which is but the Shannon entropy distribution; the monotonic coefficients in the complexity definition $C(t)$ together with the probability distribution are also used to calculate how much it spreads through K-complexity C_k -

$$\begin{aligned} C(t) &= C_k \\ &= \sum_n n p_B(n,t) \\ &= \sum_n n|\phi_n|^2 \end{aligned}$$

The dynamics of complexity in terms of the spread that is generated over the Krylov basis can also be described by the Lanczos algorithm for tridiagonalization which, as we have seen is a recursive prescription that, when applied in state space starts with an initial state and produces a sequence of states that are orthogonal to the initial state to produce a minimized Krylov basis.

Having gone through the Lanczos algorithm, the action of the hamiltonian on one of the basis produces the basis state itself together with some coefficient a_n, the next state in the basis followed by the previous state in the basis with coefficients b_n -

$$H|K_n\rangle = a_n|K_n\rangle + b_{n+1}|K_{n+1}\rangle + b_n|K_{n-1}\rangle$$

Given this outlook, the dynamics of the system are expressed out as a chain that moves from the initial state to the next, this basis tri-diagonalizes the hamiltonian which for finite dimensional systems, is known as a hessenberg form hamiltonian -

$$H = \begin{pmatrix} a_0 & b_1 & & & & \\ b_1 & a_1 & b_2 & & & \\ 0 & b_2 & a_2 & b_3 & & \\ \vdots & \vdots & \ddots & \ddots & \ddots & \\ 0 & 0 & 0 & b_n & a_n & b_{n+1} \end{pmatrix}$$

Writing out the state in its Krylov basis and coefficients -

$$|\psi(t)\rangle = \sum_n \phi_n(t)|K_n\rangle$$

the time derivative of the coefficients $\phi_n(t)$ takes on a chain form -

$$i\partial_t\phi_0(t) = a_n\phi_n(t) + b_{n+1}\phi_n(t) + b_n\phi_{n-1}(t)$$

and so as in equation (2.12), a universal one dimensional chain-type dynamic for any quantum system also holds. Using the two-point function method for spread complexity also involves the use of survival amplitudes and its relation to the partition sum and spectral form factor (SFF). The state

in Krylov basis $|\psi(t)\rangle = \sum_n \phi_n(t)|K_n\rangle$ is used to define the survival amplitude -

$$S(t) = \langle\psi(t)|\psi_0\rangle = \langle\psi_0|e^{iHt}|\psi_0\rangle$$

which generates the moments of the hamiltonian; and so if one knows the survival amplitude of the system through taking its derivatives, one can write out the moments of the hamiltonian -

$$\mu_n = \frac{d^n}{dt^n}S(t)|_{t=0} = \langle\psi_0|\frac{d^n}{dt^n}e^{iHt}|\psi_0\rangle = \langle K_0|(iH)^n|K_0\rangle$$

The moments μ_n are seen as the sum of weighted paths through an unwrapped markovian-like

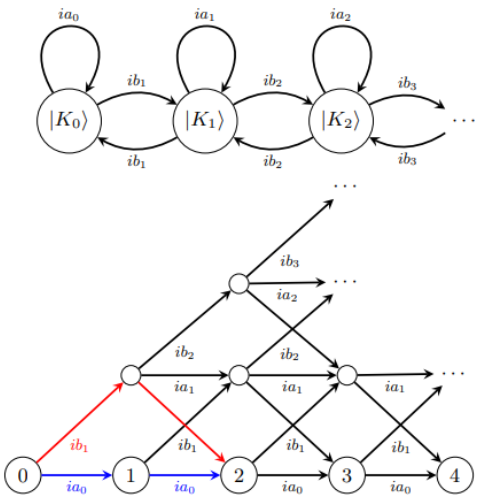

Figure 2.13: Markovian-like chain describing action of hamiltonian on $|K_n\rangle$, and the unfolding of the markovian-like chain in a time series, respectively shown with the bottom most nodes representing $|K_n\rangle$. Retrieved from [11].

graph as illustrated by the upper most image of fig 2.13; through examining the bottom figure of fig 2.13 and given that both the coefficients $\{a_0....a_{n-1}\}$ and $\{b_1...b_n\}$ are known - then a unique path within the lattice exists such that a_n contributes to the next moment μ_{n+1}, through this relation, one can recursively start from the beginning and work out every moment through knowing the survival amplitude in order to work out each of the coefficients [11].

Considering thermofield double state -

$$|\Psi_\beta\rangle = \frac{1}{\sqrt{Z(\beta)}}\sum_n e^{\frac{\beta}{2}E_n}|n,n\rangle \tag{2.21}$$

and its time evolution as in [46] -

$$|\Psi_\beta(t)\rangle = e^{-iHt}|\Psi_\beta\rangle \tag{2.22}$$

the goal of [11] included expanding the state in the Krylov basis to compute the spread complexity of the state. Given the above, the lanczos coefficients can thus be extracted from the moments using the initial thermofield double state and its time evolved state -

$$S(t) = \langle\Psi_\beta(t)|\Psi_\beta\rangle = \frac{Z(\beta - it)}{Z(\beta)} \tag{2.23}$$

this is the ratio of the analytically continued thermal partition function $Z(\beta - it) = \sum_n e^{-(\beta - it)E_n}$; and so the information needed to compute Krylov complexity for the evolution of the TFD state is captured in the quantity that has been studied extensively namely the spectral form factor (SFF) which is taken as the squared absolute value of the equation (2.23) -

$$SFF_{\beta - it} := \frac{|Z(\beta - it)|^2}{|Z_\beta|^2} \tag{2.24}$$

Another approach to studying spread complexity involves applying numerical methods to random matrix models [11]; random matrix models are known to manifests chaos, they are ubiquitous in studies that investigate the fine grained spectrum of chaotic models and are also known to have the same universal dynamics as the processes that form black holes [11, 47, 48]. Having the Hamiltonian as an $N \times N$ hermitian matrix, [11] explicitly diagonalized it into a hessenberg form and further exponentiated it in order to apply it to the corresponding Thermofield double state -

$$\frac{1}{Z(\beta)} e^{\frac{-\beta N}{4}\mathrm{Tr}[V(H)]}$$

with V denoting the potential that is invariant under unitary transformations. A generic initial state is chosen for the basis in which the matrix is drawn. Given that it is well accepted that observing the spectrum $(\lambda_1 ... \lambda_n)$ of a random $N \times N$ matrix gives the probability distribution given by -

$$P(\lambda_1 ... \lambda_n) = \Lambda_{i<j}|\lambda_i - \lambda j|^\beta e^{\frac{-\beta N}{4}\mathrm{Tr}[V(\lambda)]}$$

a relationship between the potential and the density of states also exists; extending the results from [48, 49] the hamiltonian can be tri-diagonalized and be used to derive the probability distribution -

$$P(a_o ... a_{N-1}, b_1 ... b_{N-1}) \propto \Lambda_{n=1}^{N-1} b_n^{(N-n)\beta - 1} e^{\frac{-\beta N}{4}\mathrm{Tr}[V(H)]}$$

from this, applying the exponentiated hessenberg form hamiltonian to the TFD state eliminates the need of solving the differential equation to solve for the probability distribution $\phi_n(t)$ in order to compute the krylov complexity.

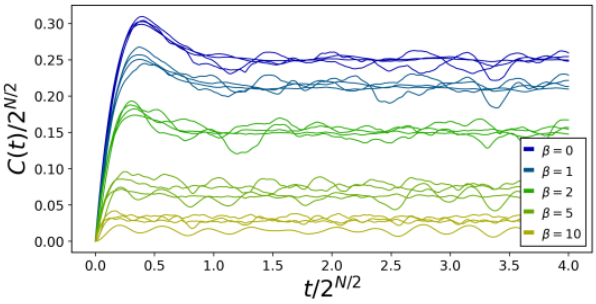

Figure 2.14: Spread complexity of TFD state in the SYK. Retrieved from [11].

The spread complexity of the TFD as illustrated in figure 2.14 displays an initial quadratic growth, an exponentially long linear ramp, a peak that's of order ae^s then a downward slope that is followed by a plateau of order be^S; these are complexity characteristics that are typically expected for chaotic systems.

To sum up - the TFD state for the SYK is built using a random hamiltonian instance from the random matrix model (Gaussian Unitary Ensemble); as from the definition of complexity, the state undergoes a recursive procedure in order to get its unitary evolution. Knowing that the recursive method will give a simplified hessenberg form, its exponentiated form is applied to an initial state to give the Krylov wave function in the Krylov basis which is used to calculate the K-complexity.

Through the first two chapters we have seen how complexity can vary in its methodology given different circumstances; and through the different case studies that were explored, it became apparent how chaos or supposed chaotic systems consistently manifested characteristics that are synonymous with the supposed complexity seen in figure 2.2. The varied examples explored in the chapters above have been predominately classified as closed systems - systems that are isolated from their environment, a connecting question further arises when it comes to understanding complexity namely; when dealing with an open system, what role does the environment contribute to the generalized characteristics of complexity?

Chapter 3

COMPLEXITY FOR OPEN QUANTUM SYSTEMS

3.1 Introduction

All quantum systems are realistically open - open quantum systems are quantum mechanical systems that are coupled to and interacting with some surrounding environment [50]; the time evolution of an isolated quantum system is typically described using the time dependant schrodinger equation while for an open quantum systems, the behaviour that is predicted by the time dependant Schrodinger equation just gives an approximation. The total hamiltonian for an open system is usually comprised of the environment, the system, some interaction and follows unitary dynamics that are described by the schrodinger equation -

$$H_{tot} = H_s + H_B + H_I$$

$$\frac{d|\Psi_t\rangle}{dt} = -iH_{tot}|\Psi_t\rangle$$

The equation for the full wave function includes both the system and the environment [51, 52], the wave function exists in the hilbert space which is large and growing exponentially with the number of degrees of freedom both in the system and environment. The challenge therein lies in the computation of the dynamics of such a wave function using standard computational devices when the whole hilbert space needs to be included.

The main interest concerns the reduced dynamics of the open quantum system hence the use of the reduced density matrix ρ_s which, is the trace over the bath or the environment degrees of freedom of the projector that is of the total wave function - $\rho_s(t) = \mathrm{Tr}_B[|\Psi(t)\rangle\langle\Psi_t|]$; this is an object where the environment degrees of freedom from the large hilbert space of the full system are traced out such that the focus is on the reduced dynamics of the system in order to obtain the evolution

equations of the open system.

The reduced dynamics are described by a universal dynamical map where an initially de-correlated state $\rho_s(0)$ and an environment/bath ρ_B that is both in equilibrium and expressed by its energy eigenstates are considered -

$$\rho_s = \rho_s(0) \otimes \underbrace{\sum_q \lambda_q |E_q\rangle\langle E_q|}_{\rho_B}$$

and without any approximations the reduced density matrix is written in terms of the dynamical map

$$\rho_s(t) = \sum_l E_l(t)\rho_s(0)E_l^\dagger(t) = \phi(t)[\rho_s(0)]$$

The map $\phi(t)$ in general is invertible, irreversible, can be written in many different operator bases such as the kraus operators $[E_l = \lambda_q\langle E_{q'}|U^{-1}(t)|E_q\rangle, (l := \{q', q\})]$ and has a time local master equation which is an evolution equation for the reduced density matrix. The dynamical map is dependant on how the environment looks like and thus models the hamiltonian that describes the interaction between the system and the environment [53].

The reduced density matrix that is expressed as a dynamical map corresponds to a trace over the environment degrees of freedom of the time evolved initial state that is assumed to be de-correlated state from the environment -

$$\rho_s(t) = \mathrm{Tr}[U^{-1}(t)\rho_s(0) \otimes \rho_B U(t)] = \phi_t[\rho_s(0)]. \tag{3.1}$$

The unitary evolution operator $U(t)$ is an evolution operator with respect to the full hamiltonian of the (system and environment) and is expressed in terms of the Dyson expansion -

$$U(t, t_0) = 1 - i\int_{t_0}^{t} dt_1 H_I(t_1) + (-i)^2 \int_{t_0}^{t} dt_1 \int_{t_0}^{t_1} dt_2 H_I(t_1)H_I(t_2) + ...$$

when plugged in the above reduced density equation (3.1) and while considering a particular interaction Hamiltonian H_I and tracing over the environment, it is noted that the reduced density matrix depends on different l order moments or different fluctuations of the coupling operator B of the environment

with respect to the initial state of the environment [53]

$$C^l(t, t_1, ..., t_l) = \mathrm{Tr}[B(t_1)...B(t_l)\rho_B].$$

Mathematically one can see that the reduced density matrix of the system will depend on the environment fluctuations or the different moments of the environment fluctuations that are in respect to the environment initial state. In terms of environments; there are two different families of environments namely statistically gaussian and non-gaussian, gaussian environments are composed of harmonic oscillators and are therefore composed of a collection of oscillators that can be of bosonic or fermionic type.

Gaussian environments have the property whereby all fluctuations can be expressed in terms of second order fluctuations and so to have a gaussian environment is to have higher order moments or higher l fluctuations that can be rewritten in terms of $l = 2$ second order moments of these fluctuations. Statistically, this is an effective property to know as it is key to describing the reduced density operator in terms of second order moments of B -

$$C(t) = \mathrm{Tr}_B[B(t)B(0)\rho_B]$$

this means experimentally if one has access to the correlation function, then one can describe the dynamics of an open system. The dynamics of the reduced density matrix can also be formulated through master equations or stochastic equations, with the Lindblad being the most used equation of motion in the field [54].

3.2 Krylov complexity

From definition, we already know that complexity entails knowing how an operator evolves through time and how complex it becomes over time; complexity thus entails knowing the dynamics of the systems and so for open quantum system, understanding and computing complexity using the Lindbladian made good research for [12]. Studying the complexity of an open quantum system using the liouvillian $\dot{\mathcal{L}} = [H, \cdot\,]$ demonstrates how differential equations do not follow as with closed systems.

The non-hermitian effects of the environment [55] on both the Von Neumann and Heisenberg equations

	Closed systems	Open systems
Von Neumann:	$\dot{\rho} = -i[H, \rho]$	$+\sum_k [L_k \rho L_k^\dagger - \frac{1}{2}[L_k^\dagger L_k \rho]]$
Heisenberg:	$\dot{O} = i[H, O]$	$+\sum_k [L_k O L_k^\dagger - \frac{1}{2}[L_k^\dagger L_k O]]$

Table 3.1: Equations of motions for different systems

as in table 3.1 are seen as an addition to the usual equation of motions thus giving a definition to the Lindbladian [54] -

$$[\dot{\mathcal{L}_f}] = [H, \cdot] - i \sum_k [L_k \dot{L}_k^\dagger - \frac{1}{2}\{L_k^\dagger L_k, \cdot\}]$$

Given a hamiltonian and a choice of Lindbladian operators L_k, the lanczos algorithm is used in principle to generate a recurrence relation for the nth operator which contributes to the computation of krylov complexity; but due to the non-hermiticity witnessed in open quantum systems a more suitable recursive algorithm namely, the arnoldi iteration, is typically ideal - for the most part it is similar to the lanczos algorithm but differentiated by the use of a non-hermitian matrix [56].

Given that the arnoldi iteration is known as a full orthogonalization procedure it is still applicable to any non-hermitian system such that, should the system be hermitian, then the underlying algorithm reduces to the lanczos algorithm.

Arnoldi iteration
For j = 0 to k-1
$h_{j,k-1} = \langle v_j \vert u_k \rangle$
$\vert u_k \rangle = \vert u_k \rangle - \sum_{j=0}^{k-1} h_{j,k-1} \vert v_j \rangle$
$h_{j,k-1} = \vert\vert u_k \vert\vert$
if $h_{j,k-1} = 0$ break, else set $\vert v_k \rangle = \frac{\vert u_k \rangle}{h_{j,k-1}}$ and proceed to step 3.

Table 3.2: Arnoldi iteration algorithm

The arnoldi coefficients $h_{j,k-1}$ as detailed in the above table, detect the dissipation effect in the system, with the diagonal elements storing information about the dissipation and the off-diagonal elements keeping track of the nature of the system whereas the lanczos coefficients are known to

not do so. [12] deduced the above observations from considering a $1d$ Transverse-Field Ising Model (TFIM) with open boundary conditions that, through jump operators [57], describe the interactions of the system with the environment without any specification of the environment detailed -

$$H_{TFIM} = -\sum_{j=1}^{N-1} \sigma_j^z \sigma_{j+1}^z - g \sum_{j=1}^{N-1} \sigma_j^x - h \sum_{j=1}^{N-1} \sigma_j^z.$$

Given some operator O, its dynamics under the Heisenberg equation is given by -

$$O(t) = e^{i\mathcal{L}_0 t}$$

and is applied to the lanczos algorithm with [12] using a vectorized form of the linbladian $\mathcal{L}_0$. The vectorization implies a change of the linbladian matrix from a $(2^N \times 2^N)$ to $(4^N \times 4^N)$ leading to a doubling of the hilbert space.

$$\mathcal{L}_0 = (I \otimes H - H^T \otimes I) + \frac{i}{2} \sum_k (I \otimes L_k^\dagger L_k + L_k^T L^* \otimes I - 2L_k^T \otimes L_k^\dagger)$$

[12] further used jump operators L with the damping amplitudes $\alpha = [0.01, 0.05, 0.1, 0.15]$ and a bulk de-phasing amplitude $\gamma = 0.1$ on a N=6 lattice site system in order to analyse the lanczos coefficients $(b_n's)$ for both the integrable and chaotic limit;

$$L_{-1} = \sqrt{\alpha}\sigma_1^+ \qquad L_0 = \sqrt{\alpha}\sigma_1^-$$
$$L_{N+1} = \sqrt{\alpha}\sigma_N^+ \qquad L_{N+2} = \sqrt{\alpha}\sigma_N^-$$
$$L_i = \sqrt{\gamma}\sigma_i^z \qquad i = 1, 2....N$$

From figure 3.1, [12] noted how the upper most figures, (a) and (b) show the growth of lanczos coefficients in an integrable and chaotic regime respectively. As the parameters γ and α are increasingly varied over large n the two figures bear similar behaviour while within a small n range, the increase of the non-hermitian parameters - γ and α, shows a deviation from hermiticity ((c) and (d) each depicting the deviation of lanczos coefficients from hermiticity). The deviation as purported by [12] is due to decoherence and not due to the chaos or integrability of the system, this then lead to the conclusion that the typical hermitian lanczos algorithm is not enough of a probe in distinguishing between an open and closed system as it is not a good enough probe

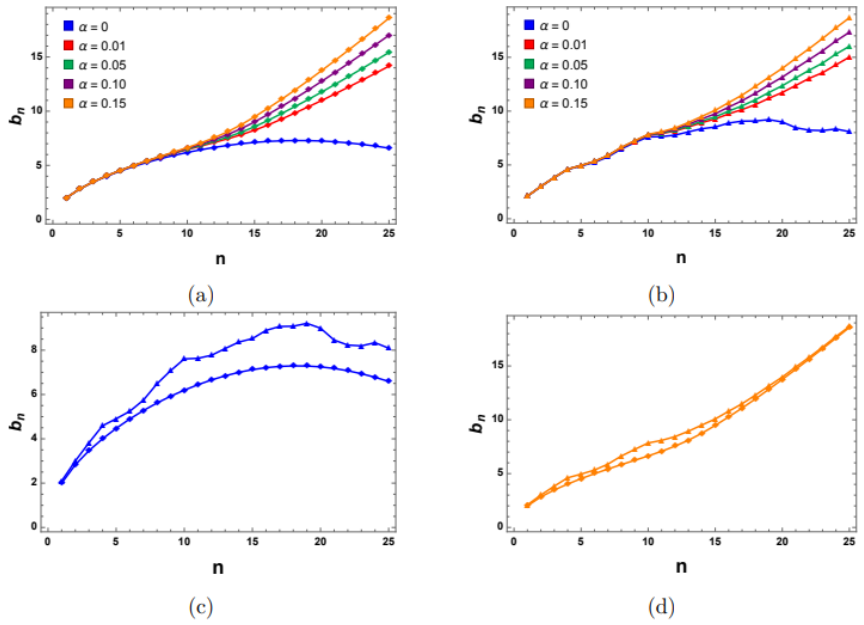

Figure 3.1: Behaviour of the lanczos coefficients of operator O located at the Z_3 site within an integrable and chaotic time limit. Retrieved from [12].

(over large n) in discerning the growth of the lanczos coefficients between integrable or chaotic regimes.

Implementing the Arnoldi algorithm gives pseudo-equivalent lanczos coefficients of an open system which are known as the arnoldi-coefficients $h_{n,n-1}$ and instead of following the typical tri-diagonal form of the hamiltonian, the arnoldi algorithm provides an alternative hessenberg matrix form [56] -

$$\mathcal{L}^o = \begin{pmatrix} h_{0,0} & h_{0,1} & h_{0,2} & \dots & h_{0,n} \\ h_{1,0} & h_{1,1} & h_{1,2} & \dots & h_{1,n} \\ 0 & h_{2,1} & h_{2,2} & h_{2,3} & \dots \\ \dots & \dots & h_{3,2} & \dots & \dots \\ 0 & \dots & \dots & \dots & h_{n-1,n} \\ 0 & 0 & \dots & h_{n,n-1} & h_{n,n} \end{pmatrix}$$

Following the arnoldi algorithm stipulated in table 3.2, the off diagonal entries just below the diagonal elements are interpreted as the norm of vectors u_k while the diagonal elements $h_{n,n}$ themselves are purely imaginary being as purported by [12] as a result of the system interacting with the environment.

Applying the arnoldi iteration to the $1d$ Transverse-Field Ising Model, the behaviour of the arnoldi

coefficients $h_{n,n-1}$ for both the integrable - fig 3.2 (a) and chaotic limit fig 3.2 (b) is seen to remain intact without any deviation and unbounded growth when there is an increase in the dissipation parameter, and so to better understand the growth of operators and distinguish whether the system is integrable or chaotic, the arnoldi iteration proved better. The downfall in the arnoldi coefficients is seen with its lack of demonstrating non-hermiticity when the dissipation parameters are increased when evaluating the growth of the difference $|h_{n,n-1} - h_{n-1,n}|$ (fig 3.2 (c),(d)) as they just seem to portray similar behaviour when parameters are increased.

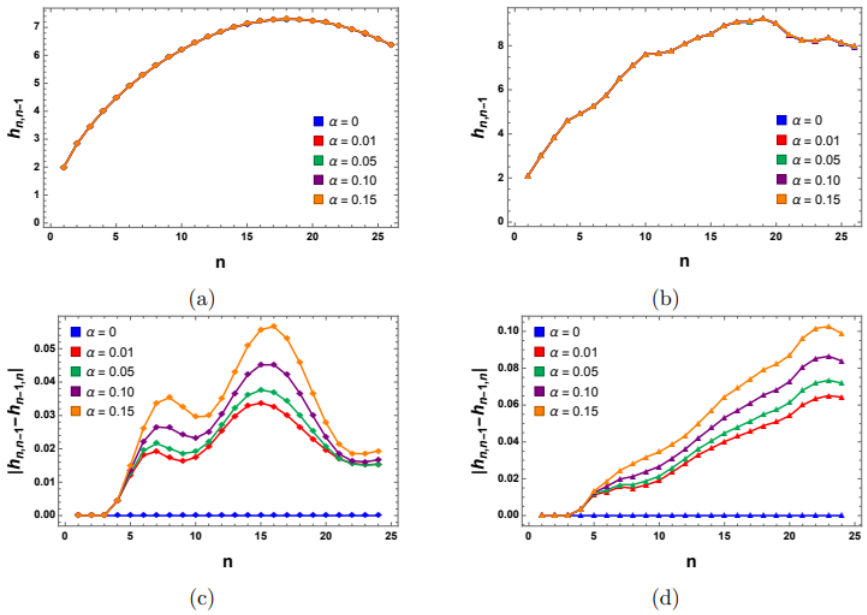

Figure 3.2: Behaviour of arnoldi coefficients of operator O located at the Z_3 site within integrable and chaotic time limits. Retrieved from [12].

Having analysed the purely imaginary off diagonal elements of the hessenberg matrix $h_{n,n}$, [12] observed a better distinction of non-hermiticity between open and closed (blue plot) systems and as such concluded on that $h_{n,n}$' are better in demonstrating non-hermiticity when the dissipation parameters are increased as pictured in figure 3.3 however, the off diagonal elements are poor in differentiating between integrability and non-integrability (seen in Fig3.4b) while the arnoldi coefficients prove to be able to discern between the two regimes as compared in figure 3.4a

[12] concluded that while the lanczos coefficients are effective for hermitian operators, when dealing with open systems that are effectively described by a Lindbladian evolution, the non-hermiticity is only well identified through using the arnoldi algorithm. The classification between an integrable

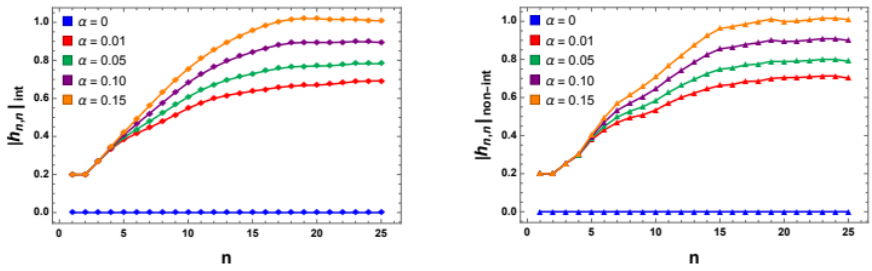

Figure 3.3: Behaviour of $h_{n,n}$ coefficients of operator O located at the Z_3 site within integrable and chaotic time limits. [12]

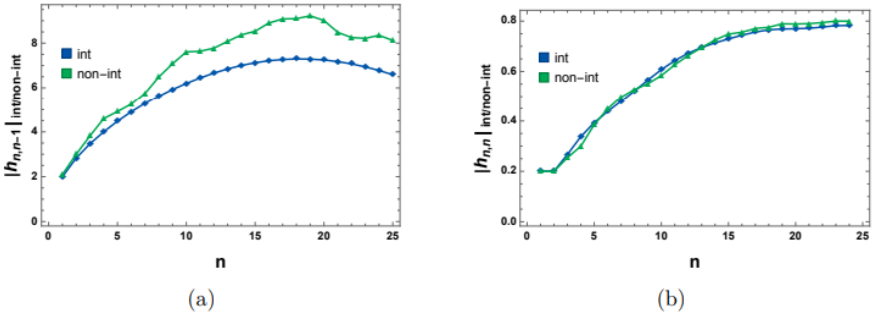

Figure 3.4: Behaviour of off-diagonal coefficients of operator O located at the Z_3 site within integrable and chaotic time limits. Retrieved from [12].

and non-integrable regime is also well differentiable when using the elements of the upper hessenberg form matrix that represents the linbladian.

Given that [12] restricted their outlook on operator growth by using the analysis of lanczos and arnoldi coefficients, a hesitancy in computing the explicit krylov complexity by [12] was noted due to the possibility of encountering computational errors caused by the loss of probability conservation on the krylov basis.

This then makes way for another outlook that can be used to compute the krylov complexity in open quantum systems; [13] explored a system coupled to a markovian bath, their results obtained are purported to be universal for all chaotic hamiltonians and are based on the statement that, the krylov complexity of an open system can be mapped to a non-hermitian tight binding model in a half infinite chain. We know that after expanding an operator/state through the krylov basis;

$$|O(t)\rangle = \rho_n(t)|K_n\rangle$$

the operator dynamics for an open system are described through the Lindbladian such that $\rho(t)$ satisfies a tight binding model - a model that describes a single particle hopping in an half-infinite chain. The same dynamics for a closed system are typically described through the Heisenberg evolution with $\rho(t)$ also being described through a tight binding model, the differentiating factor between the dynamics of an open and closed systems thus lies in the dissipation that is encoded in the open system Lindbladian consequently giving rise to the different tight binding models referenced in table 3.3.

	Tight - binding model
Closed system:	$i\partial_t \rho_n(t) = -b_{n+1}\rho_{n+1}(t) - b_n \rho_{n-1}(t)$
Open system:	$i\partial_t \rho_n(t) = -b_{n+1}\rho_{n+1}(t) - b_n \rho_{n-1}(t) - i\gamma \sum_m d_{nm}\rho_m$

Table 3.3: Mapping of a krylov complexity to a particle hopping in a half - infinite chain

For whichever open quantum model, the strength of the dissipation in the system is described by the parameter γ while the coefficients d_{nm}, give the non-hermitian terms that are mainly composed of the dissipation operators M_i and the krylov basis K_n -

$$d_{nm} = \sum_i \mathrm{Tr}[K_n^\dagger \{M_i^\dagger M_i, K_m\} \pm 2K_n^\dagger M_i^\dagger K_m M_i] \tag{3.2}$$

krylov complexity is nonetheless still defined as the average distance measured in a half infinite chain with a total weight factor of $\frac{1}{\mathcal{Z}}$ where $\mathcal{Z} = \sum_n |\rho_n|^2$ -

$$\mathcal{K}(t) = \frac{1}{\mathcal{Z}} \sum_n n|\rho_n(t)|^2.$$

Applying this new framework to both the SYK model and the one dimensional lattice model of interacting spinless fermions, [13] noticed as in figure 3.5, a similar behaviour in the diagonal coefficients d_{nn} across the board even though they dealt with different types of chaotic hamiltonians.

Referencing equation 3.2, same as in the case of increasing lanczos coefficients for chaotic hamiltonians

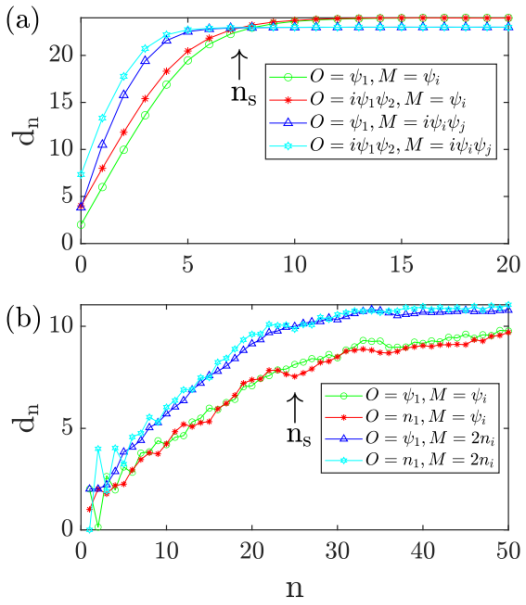

Figure 3.5: Behaviour of diagonal d_{nn} coefficients for the non-hermitian terms for both (a) the SYK and (b) 1d lattice model. Retrieved from [13].

[13] found a linear increase in the [1]d_{nn} coefficients as n increases followed by a saturation when $n > n_s$, the reasoning behind their observation depends on the supposition that; given a local operator M_i and a basis K_n acting trivially at site i, the commutation of the two does not add contribution to d_{nn} and as such only the the operator size growth of K_n (as n increases) is seen to contribute to d_{nn}. [13] further assumed that the growth behaviour of d_{nn} was $\sim n^\delta$ with $\delta = 1$ for generic chaotic hamiltonians.

Using the results from [9] that generalizes krylov complexity to being an appropriate bound of the OTOC commutator, [13] used the OTOC of a closed system at infinite temperature $\langle||[O(t), M_i]||^2\rangle$ together with the krylov complexity $\mathcal{K}(t)$ to support their claim on the growth behaviour of d_{nn};

$$\begin{aligned}\sum_i \langle||[O(t), M_i]||^2\rangle &= \sum_i \langle||[\sum_n \rho_n(t)^c K_n, M_i]||^2\rangle \\ &\approx \sum_i \sum_n |\rho_n(t)^c|^2 \langle||[K_n, M_i]||^2\rangle \\ &= \sum_n |\rho_n(t)^c|^2 d_{nn} \leq \mathcal{C}\mathcal{K}(t)\end{aligned}$$

[1] when m=n, this gives the diagonal elements $d_{nn} = \sum_i \mathrm{Tr}[[K_n, M_i]^\dagger [K_n, M_i]]$

Knowing that $\mathcal{K}(t) = \frac{1}{\mathcal{Z}} \sum_n n|\rho_n(t)|^2$ then -

$$\sum_n |\rho_n(t)^c|^2 d_{nn} \leq \mathcal{C}\mathcal{K}(t) = {}^2\mathcal{C} \sum_n n|\rho_n(t)|^2$$

For the bound to hold then $\delta < 1$, with the bound being a supremum when $\delta = 1$, leading [13] to conclude that a linear increase of the coefficients d_{nn} exists. Beyond using the behaviour of the coefficients to distinguish the chaoticity of the system, the spectrum of the non-hermitian tight binding model is known to play a crucial role in describing the dynamics of the krylov complexity with the time evolution being denoted as follows -

$$\rho(t) = \sum_l c_l e^{-i(\epsilon_l' - i\epsilon_l'')t\phi_l}$$

When the dissipation parameter is larger than some dissipation constant ($\gamma > \gamma_c$), the eigen-state ϕ_l and the respective eigen-energies $\{\epsilon_l', \epsilon_l''\}$ display a gap in the eigen-energies $\epsilon = \epsilon' - i\epsilon''$ as noted in fig 3.6 (b), the two modes that are noted below the gap are known to produce wave functions $|\phi(n)|^2$ that are localized at the edge of the half - infinite chain - a characteristic believed by [13] to be exhibited by non hermitian tight bonding models as seen in fig 3.6(c).

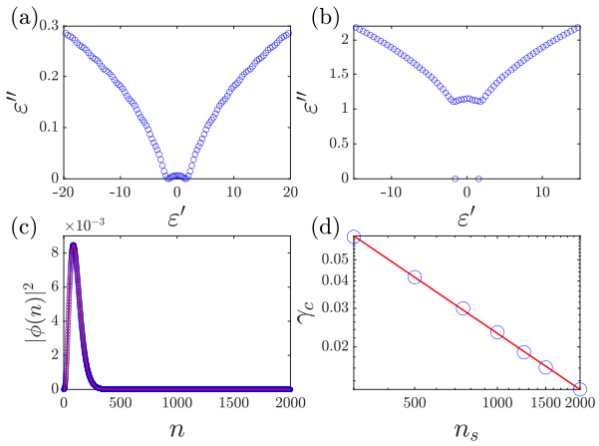

Figure 3.6: (a,b) eigen-energies for $\gamma = 0.007 < \gamma_c$ and $\gamma = 0.04 > \gamma_c$ respectively. (c) wave functions of 2 modes below gap and (d) behavior of γ_c with n_s. Retrieved from [13].

The two localized modes are further noted to have ascendancy over the long time evolution of ρ such that the krylov complexity is seen to saturate to a much smaller value than that typically witnessed in closed systems with the same hamiltonians, leading to the conclusion that dissipation suppresses the growth of complexity as illustrated in fig 3.7.

[2] $\mathcal{C}$ being some constant

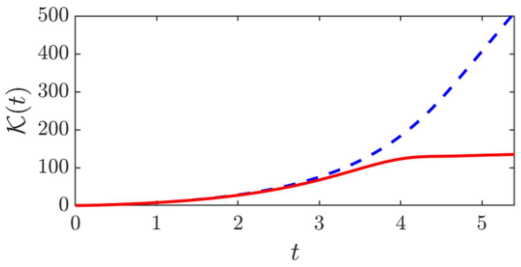

Figure 3.7: krylov complexity in open systems (red) compared to that seen in closed systems. Retrieved from [13].

3.3 Circuit complexity

Section 3.2 detailed the different methods that have so far been used in understanding krylov complexity within an open quantum system, these methods have shown the role that the environment and dissipation play on the growth of krylov complexity; following from the investigations done in computing circuit complexity under closed quantum systems, we extend the study of circuit complexity under open systems with the use of other regimes namely - Complexity of Purification (COP) and Operator state mapping [14].

3.3.1 Complexity of purification

Complexity in QFT is interpreted as the difficulty associated in preparing a state $|\psi_T\rangle$ $l = l$ via a unitary transformation $\hat{U}$ from a pure, typically disentangled reference state $|\psi_R\rangle$, a question then arises as to what quantum information and properties are held by mixed states.

When one has a pure system, entanglement is typically a good measure of quantum correlation, but when one has a mixed system like an open quantum system then entanglement entropy is not a good measure of quantum correlation resulting in the use of entanglement purification [58]. Complexity of purification is an analogue of entanglement purification; and so while complexity is for a closed system, complexity of purification is a process similar in thought as the entanglement purification to compute the complexity for open quantum systems [14].

Complexity of purification [59] generalizes the notion of pure state complexity to mixed states - given a mixed state ρ_A in some Hilbert space $\mathcal{H}_A$, a new enlarged Hilbert space with an ancillary

system A' is defined -

$$\mathcal{H} = \mathcal{H}_A \otimes \mathcal{H}_{A'}$$

many purifications $|\psi_T\rangle$ thus exist in $\mathcal{H}$ such that once the ancillary is traced out, the original density matrix is recovered and defined as -

$$\rho_A = \mathrm{Tr}_{\mathcal{H}_{A'}}(|\psi_t\rangle\langle\psi_t|)$$

Complexity of purification is then defined as the minimum of complexity $\mathcal{C}$ with respect to a reference state $|\psi_R\rangle$ and to all possible purifications $|\psi_T\rangle$ -

$$\mathcal{C}_P[\rho_A] = \min_{|\psi\rangle\in\mathcal{H}}\mathcal{C}(|\psi_R\rangle, |\psi_T\rangle).$$

[14] considered both the harmonic oscillator and pseudo-chaotic toy model represented by the inverted harmonic oscillator when using COP; for the harmonic oscillator, they investigated the behaviour of complexity when the bath interacts with the system and when the system transitions from being under-damped to being over-damped while for the inverted harmonic oscillator, [14] wanted to understand how the environment can affect the unstable fixed point typically found in an inverted harmonic oscillator and if complexity can be used to regulate chaotic-like behaviour.

The system at hand is represented by the harmonic oscillator while the environment/bath is represented by a one dimensional free bosonic field theory, resulting in the defined hamiltonian [60]

-

$$H = \int_0^L dx\left\{\frac{1}{2}(\Pi^2 + (\partial_x\phi_R)^2) + \delta(x) + \left[\frac{1}{2}P^2 + \frac{w_0^2}{2}Q^2 + 2\lambda Q\partial_x\phi_R\right]\right\}$$

with both the system variables $[Q, P]$ and the fields $[\phi(x), \Pi(x')]$ being canonically conjugate. Having considered the hamiltonian under a quench protocol,

$$H = \begin{cases} H_<, & t < 0 \\ H_>, & t > 0 \end{cases} \tag{3.3}$$

$H_>$ is used to evolve the system and to get the final state $|\psi(t)\rangle = \exp(-iH_>t)|\psi(0)\rangle$ while $H_<$ gives the hamiltonian for both the system and bath when decoupled and is used to attain the ground state

-

$$H_< = \int_0^L dx \Big\{ \underbrace{\frac{1}{2}(\Pi^2 + (\partial_x \phi)^2)}_{H_B} + \underbrace{\frac{1}{2}(P^2 + \Omega_<^2 Q^2)}_{H_S} \Big\}$$
$$= \sum_{n=1}^{\infty} \Omega_n \left(a_n^\dagger a_n + \frac{1}{2} \right) + \Omega_< \left(a_0^\dagger a_0 + \frac{1}{2} \right)$$

with the following terms in mode expansions -

$$Q = \frac{1}{2\Omega_<}(a_0 + a_0^\dagger)$$
$$P = -i\sqrt{\frac{\Omega_<}{2}}(a_0 - a_0^\dagger)$$
$$\phi(x) = \sqrt{\frac{2}{L}} \sum_{n=1}^{\infty} \sin\left(\frac{n\pi}{L}x\right)\left(\frac{1}{\sqrt{2\Omega_n}}\right)(a_n + a_n^\dagger)$$
$$\Pi(x) = -i\sqrt{\frac{2}{L}} \sum_{n=1}^{\infty} \sin\left(\frac{n\pi}{L}x\right)\left(\sqrt{\frac{\Omega_n}{2}}\right)(a_n - a_n^\dagger)$$

The hamiltonian describing the environment/bath when introducing a dual field $\Pi(x) = -\partial_x \theta$ becomes represented as follows -

$$H_B = \int_0^L dx \frac{1}{2}[(\partial_x \theta)^2 + (\partial_x \phi)^2]$$

where the fields ϕ and θ are translated into left and right movers that satisfy the commutation relation rules.

$$\phi(x) = \phi_R(x) + \phi_L(x)$$
$$\theta(x) = \theta_R(x) + \theta_L(x)$$

Applying the dirichlet boundary conditions on the fields leads to an implication that ϕ_L is a continuation of ϕ_R when $x < 0$, using this, the Hamiltonian can be written in terms of right movers and the equations of motion -

$$H = \int_{-L}^{L} dx \Big\{ ((\partial_x \phi_R)^2) + \delta(x) + \left[\frac{1}{2}P^2 + \frac{w_0^2}{2}Q^2 + 2\lambda Q \partial_x \phi_R \right] \Big\}$$

Knowing that the right movers of the field equation are functions of (x, t) and limiting their range of integration about $(x = 0)$, [14] further denoted $\phi_R^+(x) := \phi_R(x > 0)$ and $\phi_R^-(x) := \phi_R(x < 0)$ to

simplify the equations of motion of the operators -

$$\partial_t \phi_R = -\partial_x \phi_R - \delta(x)\lambda Q \qquad \longrightarrow \qquad 0 = \phi_R^+(x=+\epsilon) - \phi_R^-(x=-\epsilon)|_{\epsilon\to 0} + \lambda Q \tag{3.4}$$

$$\frac{d^2Q}{dt^2} = -w_0^2 Q - 2\lambda \partial_x \phi_R(0) \qquad \longrightarrow \qquad \frac{d^2Q}{dt^2} + w_0^2 Q = -\lambda[\partial_x \phi_R^+(x=0) + \partial_x \phi_R^-(x=0)] \tag{3.5}$$

Solving for the differential equation involving Q (equation 3.5) includes splitting it into both its homogeneous and particular parts, such that the homogeneous section is solved through the typical differential methods while a Fourier transform is performed for the particular solution of Q.

$$\begin{aligned} Q(t) &= Q_H(t) + Q_P(t) \\ &= e^{-\Gamma t}\left\{[\cos\Omega t + \frac{\Gamma}{\Omega}\sin\Omega t]Q(t=0) + \frac{1}{\Omega}\sin\Omega t P(t=0)\right\} - \\ &\quad e^{-\Gamma t}\left\{[\cos\Omega t + \frac{\Gamma}{\Omega}\sin\Omega t]Q_P(t=0) + \frac{1}{\Omega}\sin\Omega t \dot{Q_P}(t=0)\right\} + \left(\frac{i2\sqrt{2\Gamma}w}{w^2 + i2\Gamma w - w_0^2}\right)\phi_R^- \end{aligned}$$

The differential equation for the field/bath in terms of right movers is given by -

$$\phi_R^+(w) = -\sqrt{2\Gamma}Q_H(w) + \left(\frac{w^2 - i2\Gamma w - w_0^2}{w^2 + i2\Gamma w - w_0^2}\right)\phi_R^-(w)$$

with the damping variables defined as $\Gamma = \frac{\lambda^2}{2}$ and $\Omega = \sqrt{w_0^2 - \Gamma^2}$. Getting the reduced density matrix of the system/oscillator involves tracing out the bath/environment/string $\hat{\rho_S} = \mathrm{Tr}_B[\hat{\rho}]$ -

$$\begin{aligned} \hat{\rho_S} &= \mathrm{Tr}_B[\hat{\rho}] \\ &= \int dx dx' \rho_S(x,x')|x\rangle\langle x'| \\ &= \int dx dx' \int \Pi_i dq_i \rho(x,\{q_i\}|x',\{q_i\})|x\rangle\langle x'| \\ &= \int dx dx' \int \Pi_i dq_i \psi(x,q_i)\psi^*(x',q_i')|x\rangle\langle x'| \end{aligned}$$

In position representation, the density matrix of the system through time is defined as follows -

$$\rho_S(x,x') = \sqrt{\frac{\gamma_1 - \eta}{\pi}} \exp\left\{ -\frac{\gamma}{2}x^2 - \frac{\gamma^*}{2}x'^2 + \eta x x' \right\} \tag{3.6}$$

$$\gamma = \gamma_1 + i\gamma_2 \in \mathbf{C}, \eta \in \mathbf{R} \tag{3.7}$$

Knowing that correlation functions can be produced from reduced density matrices, the parameters γ, η can thus also be reproduced from correlation functions [14],

$$\begin{aligned}
\gamma_1 &= \sigma_P - \frac{1}{\sigma_Q}(\sigma_Q^2 - \frac{1}{4}) \\
\gamma_2 &= -\frac{\sigma_{QP}}{\sigma_Q} \\
\eta &= \sigma_P - \frac{1}{\sigma_Q}(\sigma_Q^2 + \frac{1}{4})
\end{aligned}$$

defined by its first and second moments with the moments of any order being derived from a characteristic function; $\langle O^l(t)\rangle \frac{\partial^l}{\partial(i\epsilon)^l} CF(\epsilon,t) = \frac{\partial^l}{\partial(i\epsilon)^l} \mathrm{tr}(\rho \exp -i\eta(\epsilon a + \epsilon^* a^\dagger))$ -

$$\begin{aligned}
\sigma_Q &= \langle Q(t)Q(t)\rangle = \frac{1}{2(\gamma_1 - \eta)} \\
\sigma_P &= \langle P(t)P(t)\rangle = \frac{|\gamma|^2 - \eta^2}{2(\gamma_1 - \eta)} \\
\sigma_{QP} &= \frac{1}{2}\langle Q(t)P(t) + P(t)Q(t)\rangle = -\frac{\gamma_2}{2(\gamma_1 - \eta)}.
\end{aligned}$$

Once one has the reduced density matrix, complexity of purification can then be applied in order to see the effects of the bath on the system. Following the purification used in [61, 62, 63], [14] chose an ancillary system to represent the total system in size, with the subsystem at hand being the oscillator. The pure wave function consequently has a parametrized structure in position representation -

$$\psi(x, x_{anc}) = \mathcal{N} \exp\{-\frac{1}{2}(\alpha x^2 + \beta x_{anc}^2 - 2\tau x x_{anc})\}$$

The reduced density matrix of the system at hand, after tracing out the ancillary hilbert space is given by -

$$\hat{\rho}_S = \mathrm{Tr}_{anc}[\rho(x, x_{anc}|x, x'_{anc})] \tag{3.8}$$

$$= \int_{-\infty}^{\infty} dx_{anc}\psi(x, x_{anc})\psi^*(x', x'_{anc}) \tag{3.9}$$

$$= \mathcal{N}^2 \exp\left\{ -\frac{1}{2}\left[\left(\alpha - \frac{\tau^2}{2\mathrm{Re}(\beta)}\right)x^2 + \left(\alpha^* - \frac{(\tau^*)^2}{2\mathrm{Re}(\beta)}\right)x'^2\right] + \left(\frac{|\tau^2|}{2\mathrm{Re}(\beta)}\right)xx'\right\} \tag{3.10}$$

Through the matching of equation 3.6 to equation 3.10, the values of $[\alpha, \mathrm{Re}(\beta), \tau]$ are evaluated as -

$$\alpha = \sigma_P$$

$$\mathrm{Re}(\beta) = 2\sigma_Q$$

$$\tau^2 = 4\sigma_{QP}^2 - 1 + 4i\sigma_{QP}.$$

Applying the same method used when computing circuit complexity (as seen in chapter 2.3.1); the reference state for the system is defined by using the aforementioned pure wave function ($\psi(x, x_{anc})$), when taking into account the assumption imposed by [14] that $\langle Q\rangle = 0$ and $\langle P\rangle = 0$ for the initial wave function this simplifies the pure wave function even further to give - $\psi_r \sim \exp\{-\frac{1}{2}w_r(x^2 + x_{\mathrm{anc}}^2)\}$. The reduced density matrix $\hat{\rho}_{\mathrm{S}}$ is defined as the target state; using the two states, the complexity is then calculated to give -

$$\mathcal{C}(\psi) = \sqrt{\sum_i^2 \left[\ln\left(\frac{|w_i|}{w_r}\right)^2 + \tan^{-1}\left(-\frac{\mathrm{Im}(w_i)}{\mathrm{Re}(w_i)}\right)^2\right]}$$

with

$$w_1 = \frac{1}{2}(\alpha + \beta + \sqrt{(\alpha - \beta)^2 + 4\tau^2})$$

$$w_2 = \frac{1}{2}(\alpha + \beta - \sqrt{(\alpha - \beta)^2 + 4\tau^2})$$

$$w_r = 1.$$

Since complexity of purification is the minimum of the complexity $\mathcal{C}$, the minimization of the above complexity when carried over to Im(β) [14] gives the following complexity of purification -

$$\mathcal{C}_\rho = \min_{\mathrm{Im}}\left(\sqrt{\sum_i^2\left[\ln\left(\frac{|w_i|}{w_r}\right)^2 + \tan^{-1}\left(-\frac{\mathrm{Im}(w_i)}{\mathrm{Re}(w_i)}\right)^2\right]}\right)$$

and so for the harmonic oscillator, the complexity of purification given by the different damping

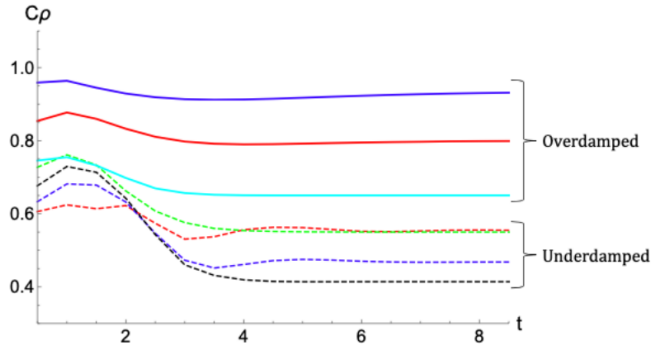

Figure 3.8: complexity of purification for a harmonic oscillator in an open system with different damping values Γ. Retrieved from [14].

values is seen to generally saturate overtime. The smaller the value of the damping compared to the initial frequency w_0 leads to an under-dampening of the system while, if the damping parameter is greater than the initial frequency, the oscillator is over-damped as seen in Fig 3.8. The increase of the damping parameter within the under-damped regime of $\Gamma^2 < w_0^2$ brings with it a kink irregularity when analysing the saturation values of the complexity of purification.

Continuing with the same train of thought for analysing the complexity of chaos-characterized systems, the complexity of purification for the inverted harmonic oscillator is differentiated from the harmonic oscillator by a complex initial frequency iw_0 used in the definition of canonically conjugate variable Q that describes the system.

Figure 3.9 shows the complexity of purification through time for different damping parameters Γ with the red graph representing the lowest value of damping used and cyan the greatest, for all values of damping applied, a general linear growth is witnessed correlating with literature in that the growth of complexity witnessed in chaotic systems, more so for the inverted harmonic oscillator as studied in [64] is linear.

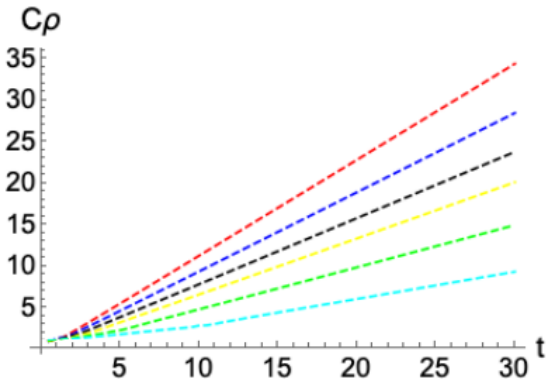

Figure 3.9: complexity of purification for an inverted oscillator in an open system with different damping values Γ. Retrieved from [14].

The isolated inverted harmonic oscillator has an unstable fixed point that is used to characterize its chaotic-like behaviour [14] noticed the role of how varying the damping parameter Γ contributed to the regulation of the system. Starting from a low valued Γ, the slope of the complexity of purification is large and seen to grow linearly, with it decreasing in slope angle as the value of damping is increased (as illustrated in Fig 3.9).

The more damping and interaction is introduced to the inverted system it seems that, while still growing in a linear manner, a decrease in the rate of growth of the complexity of purification is observed, implying an effect that the damping/interaction has on adjusting the instability of the system.

3.3.2 Complexity by operator state mapping.

Operator state mapping is another diagnostic tool that is used to compute the circuit complexity, it involves taking an operator $\hat{O}$ with a matrix representation and orthornormal basis $\{|m\rangle\}$ and mapping it to give a corresponding state that will be used as the target state [65, 66] -

$$\hat{O} = \sum_{m,n} \hat{O}_{m,n} |m\rangle\langle n| \longleftrightarrow |\hat{O}\rangle = \frac{1}{\sqrt{\mathrm{Tr}[\hat{O}^\dagger \hat{O}]}} \sum_{m,n} \hat{O}_{m,n} |m\rangle_{in} \otimes |n\rangle_{out}$$

[14] also included in their study of the complexity for open quantum system the circuit complexity through operator state mapping, which mapped the reduced density matrix $\hat{\rho_S}$ to a state in a doubled

Hilbert space -

$$\hat{\rho_{\rm S}} = \int dxdx' \rho_{\rm S}(x.x')|x\rangle\langle x'| \longleftrightarrow \int dxdx' \rho_{\rm S}^{\frac{1}{2}}(x.x')|x\rangle_{in} \otimes |x'\rangle_{out}$$

The corresponding wave function in the doubled Hilbert space will be used as the target state in computing the complexity -

$$\begin{aligned}\psi(x,x') &= \rho_{\rm S}^{\frac{1}{2}}(x.x') \\ &= \left(\frac{\gamma_1^2-\eta^2}{\pi^2}\right)^{\frac{1}{4}} \exp[-\frac{1}{2}\Big(\gamma+\eta\Big)x^2 - \frac{1}{2}\Big(\gamma^*+\eta\Big)x'^2 + \sqrt{2\eta(\gamma_1+\eta)}xx']\end{aligned}$$

To further simplify the effective wave function the arguments found within the exponential are diagonalized using a basis $\{X, X'\}$ [14] -

$$\psi(x,x') = \left(\frac{\gamma_1^2-\eta^2}{\pi^2}\right)^{\frac{1}{4}} \exp\Big[-\frac{1}{2}(\xi_1+E)X^2 - \frac{1}{2}(\xi_1-E)X'^2\Big]$$

whereby

$$\begin{bmatrix} X \\ X' \end{bmatrix} = \begin{bmatrix} u & -v \\ v & u \end{bmatrix} \begin{bmatrix} x \\ x' \end{bmatrix}$$

$$u = \sqrt{\frac{1}{2}(1+i\frac{\xi_2}{E})} \qquad \xi_1 = \mathrm{Re}[\gamma+\eta]$$
$$v = \sqrt{\frac{1}{2}(1-i\frac{\xi_2}{E})} \qquad \xi_2 = \sqrt{\kappa^2-E^2}$$

circuit complexity from the Operator state mapping for the open system doesn't seem as much as a good probe of complexity for both the typical and inverted oscillator, the linear growth that is expected for chaotic systems (for the inverted oscillator) was not apparent as seen in figure 3.10, only a general saturation dominating through for all the different damping parameter values was noted. The lack in the probe sensitivity of the Operator state mapping is, as proposed by [14] due to the lack of a tracing minimization method seen in the complexity of purification procedure, this then continues the search for methodologies that could be better probes of complexity in open quantum systems.

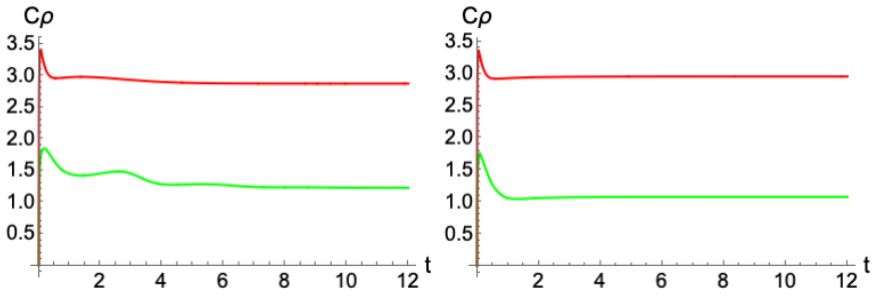

Figure 3.10: complexity of purification for an inverted oscillator in an open system with different damping values Γ. Retrieved from [14].

3.4 Krylov complexity for non gaussian random matrix model random matrix model with noise

This chapter will make some progress by extending investigations towards a new open quantum system, applying part of the techniques mentioned in previous chapters to compute complexity; in this section we will in part study the effects of the environment on both the spectral form factor and Krylov complexity of two models namely;

- The random matrix theory (RMT) with an addition of noise as our base model.
- Non - gaussian random matrix theory with quartic and sextic potential terms.

with both models being drawn from [67]. RMT's are typically characterized by a ramp time scale - a time scale that distinguishes energy correlations, the energy levels below the ramp time scale are believed to portray no correlation while the energy levels above the ramp time display correlations. The spectral form factor SFF is then the primary tool that is able to probe both the timescales and spectra of such systems [68, 69, 70] and as seen in chapter 2, the relation that the SFF has to the auto correlation function makes it an important element that can also be used in computing the krylov complexity for the open system.

3.4.1 The spectral form factor

The environment is part of the key definition of an open quantum system, and so the effects that the environment has on the SFF has an analogue given by the fidelity of a coherent Gibbs state $|\psi_\beta\rangle = \sum_{n=1}^{d} \frac{e^{-\beta E_n/2}}{\sqrt{\mathrm{Tr}[e^{-\beta H_0}]}}|n\rangle$ and its time evolution [71, 72], the simplified fidelity as seen in [73] is

given by -

$$F(t) = \langle\psi_\beta| \underbrace{\rho(t)}_{\text{density matrix}} |\psi_\beta\rangle$$

$$F(t) = \langle\psi_\beta| \underbrace{\Lambda[\rho(0)]}_{\text{time evolution described with the use of a quantum channel}\Lambda^{3}} |\psi_\beta\rangle$$

$$F(t) = \langle\psi_\beta|\Lambda[|\psi_\beta\rangle\langle\psi_\beta|]|\psi_\beta\rangle$$

$$F(t) = \left|\frac{Z_0(\beta+it)}{Z_0(\beta)}\right|^2$$

Following [71, 72], expressing the above fidelity function in terms of a partition function that has been continued to complex inverse temperature simplifies the process in acquiring the SFF for both our gaussian and non-gaussian model.

$$F(t) = \sqrt{\frac{1}{4\pi\gamma t}}\int_{-\infty}^{\infty} dy e^{\frac{-y^2}{4\gamma t}} \underbrace{\left|\frac{Z_0(\beta+i(y+t))}{Z_0(\beta)}\right|^2}_{\text{Systems SFF}} \tag{3.11}$$

- SFF for the gaussian RMT with noise:

  Most gaussian matrix ensembles consist of matrices that have random entries that have been drawn from a gaussian distribution, the joint probability distribution of these is then given by [67]:

  $$P(M)dM = \exp\left(\frac{-1}{2}\text{tr}M^2\right)dM \tag{3.12}$$

  the equation above thus allows for any ensemble of matrices to be chosen meaning that the random elements of the matrix can be drawn from any ensemble[67], an ensemble that is typically used to describe a time dependent RMT is given by:

  $$Z = \int dM e^{-\text{Tr}(V(M))} \tag{3.13}$$

  with $V(M)$ being the system's potential which, for the gaussian RMT is given by $V = \frac{1}{2}M^2$. The ensemble explicitly expressed in the eigenvalues of the matrix is written out as [67] -

  $$Z = \Pi_{i=1}^{N}\int d\lambda_i e^{-N\sum_i^N V(\lambda_i)+\beta\sum_{i<j}^N \log(\lambda_i-\lambda_j)}$$

  The reliance of the spectral form factor on the random matrix theory follows in the definition

[3] A positive linear mapping from density operators to density operators and is also trace preserving [74]

of the spectral form factor getting its definition as a partition function that has been analytical continued [67] -

$$|Z(\beta+it)|^2 = \sum_{m,n} e^{-\beta({E_m}^4+E_n)} e^{-it(E_m-E_n)} \tag{3.14}$$

given the polynomial potential $V(M)$, the SFF is then averaged over the matrix ensembles to better analyse the characteristics associated with quantum chaos -

$$SFF_{average} = G(\beta,t) = \frac{\langle |Z(\beta+it)|^2 \rangle}{\langle Z(\beta) \rangle^2} \tag{3.15}$$

- SFF for non gaussian RMT with noise:

  Viewing the non-gaussian RMT as a deformed gaussian [67], we take the results from [67] and extend the investigation towards the non-gaussian spectral form factor to observe the effects that the environment has on the system's SFF ramp time scale in order to compare it to the gaussian spectral form factor (base model). The potential used for the non-gaussian RMT used in defining the SFF is differentiated by the presence of both quartic and sextic terms -

$$V(M) = \frac{1}{2}M^2 + \frac{g}{N}M^4 + \frac{h}{N^2}M^6$$

While the spectral form factor and its average can be attained analytically as seen in [67], a numerical alternative was used for this project. Figure 3.11 exhibits the averaged SFF of both models, the effects of non-gaussianity are noticed to change the minimum time and ramp slope, with no affect on its late time behavior.

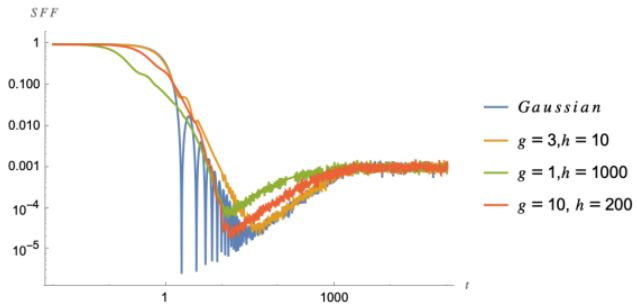

Figure 3.11: Averaged Spectral form factor for both the gaussian potential (blue) and non gaussian potential with varied parameters g/h.

[4] eigenvalues from the potential V(M)

The obtained SFF results are then used in the defined fidelity equation (3.12) in order to see the effects of the environment on both models as captured in figure 3.12 and figure 3.13.

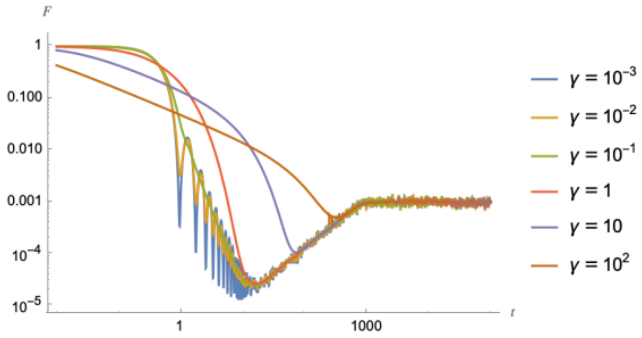

Figure 3.12: Averaged gaussian spectral form factor affected by the environment.

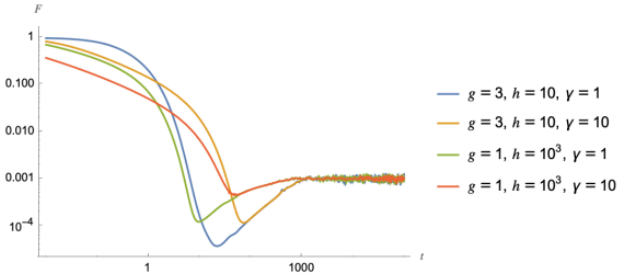

Figure 3.13: Averaged non-gaussian spectral form factor influenced by the environment.

The classic dip-ramp time scale (a typical characterization of a chaotic system) is witnessed even when including noise to both models, the late time behaviour for both the gaussian and non-gaussian is also the same due to the eigenvalue correlation that exists at short distances [75] - seen in figure 3.12 and figure 3.13.

It is noticed that, the greater the value of the parameter [5]γ the lesser the length of the ramp time scale, while non-gaussianity has been shown to have an early dip time in figure 3.11, the dip time becomes greatly differentiable when the parameter γ is increased - the greater the parametric value, the greater the dip time.

the dip time is used to see when the ramp behaviour begins, the ramp time on the other hand is

[5]strength dephasing parameter seen in equation 3.11

known to be a key indicator of the differences in the nearest-neighbor energy eigenvalues of the SFF and so, knowing the dip time and how it is affected by the environment speaks into the emergence of random matrix behavior in a quantum chaotic system and how its affected by the environment. To conclude - from figure 3.13, the greater the effect of the γ within the system then this delays the occurrence of the typical effects of the RMT.

Taking the above results in hand, the relation between the SFF and krylov complexity already implies a dampening effect that the environment could have on the complexity which will be numerically explored in the following section.

3.4.2 Complexity Results

The Quantum mechanical state of any system evolves through time according to the Schrodinger equation:

$$i\partial_t|\psi(t)\rangle = H|\psi(t)\rangle$$

with the state of the system at the time t being given by -

$$\begin{aligned}|\psi(t)\rangle &= \sum_{n=0}^{\infty} \frac{(-it)^n}{n!}|\psi_n\rangle \\ &= \sum_{n=0}^{\infty} \frac{(-it)^n}{n!}H^n|\psi(0)\rangle\end{aligned}$$

Using the Gram-Schmidt procedure on the basis $|\psi_n\rangle$ normalizes and generates an orthogonal basis $\mathcal{K}$ that expands the subspace of the Hilbert space explored by the evolution of the initial state $|\psi(0)\rangle := |K_0\rangle$

$$\mathcal{K} = \{|K_n\rangle : n = 0, 1, 2, ...\}$$

The procedure also tri-diagonalizes the hamiltonian (when H hermitian) on the basis and as such expressing the H on the basis simplifies the state -

$$|\psi(t)\rangle = \sum_{n=0}^{\infty} \phi_n(t)|K_n\rangle$$

which is used in part to define krylov complexity -

$$C(t) = C_{\mathcal{K}}(t) = \sum_n n|\phi_n(t)|^2$$

Evaluating the tri-diagonalized hamiltonians of the matrix models we are investigating, then the growth of complexity for the models, differentiated by the different values of g and h, is illustrated in fig 3.14. We see that the effect of the non-gaussian terms in the Hamiltonian, when compared to

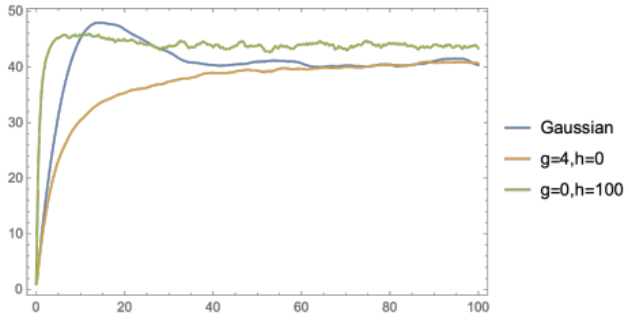

Figure 3.14: Growth of complexity of gaussian and non-gaussian RMT model through time.

the gaussian hamiltonian (base model), changes the initial slope growth and also the initial point of saturation, but after time, the saturation value tends to be the same for the different models.

Taking the role of the environment into account for both the gaussian and non gaussian model includes the use of the Lindbladian, which uses the evolution operator ($e^{-it\mathcal{L}_0}$) instead of (e^{-itH}). From [12] we know that the operator can act on a doubled Hilbert state constructed from the density matrix and is represented by -

$$\mathcal{L}_0 = (I \otimes H - H^T \otimes I) + \frac{i}{2}\sum_k (I \otimes L_k^\dagger L_k + L_k^T L^* \otimes I - 2L_k^T \otimes L_k^\dagger)$$

Where H represents the aforementioned closed system Hamiltonian for either the gaussian or non-gaussian model. Taking a simple consideration that there be γ number of the jump operators L_k depending on the hamiltonian according to a function w [72] -

$$\begin{aligned} L_k &= w(H) \\ &= H^\delta \end{aligned}$$

The result of complexity evolution for the different parameters γ and for the case $\delta = \frac{1}{2}$ is given by figure 3.15

We see that the introduction of noise in the system causes an initial sharp increase but followed by an exponential decay at later time. Instead of the lindbladian, the evolution can also be represented

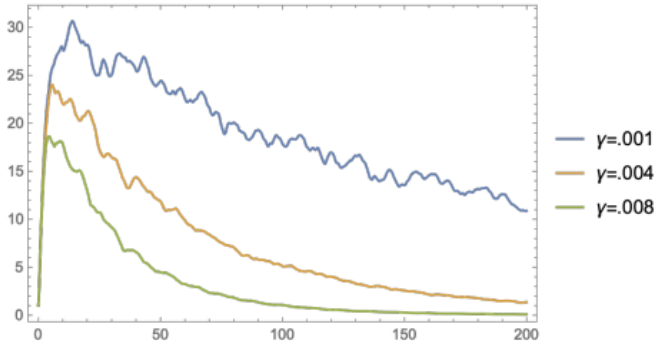

Figure 3.15: Growth of complexity for open gaussian model.

by an effective hamiltonian [72] -

$$H_{eff} = H_0 - i\gamma w(H_0)^\dagger w(H_0)$$

For this case, we also define the complexity to be given by the components of the state vector at time t in the krylov basis. The comparison of the effect of noise and non-gaussianity of the system on the growth complexity for the models is illustrated in figure 3.16.

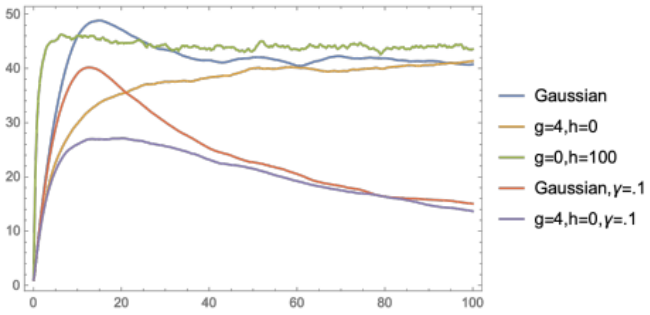

Figure 3.16: Growth of complexity of open gaussian and non-gaussian model through time.

While the generalized characteristics of quantum complexity for both models in figure 3.16 are noted i.e. - an initial quadratic growth, an exponentially long linear ramp, a peak, downward slope followed by a plateau, the introduction of the strength de-phasing parameter γ causes a decrease in the generalized slope characteristics for complexity.

Analysing figure 3.16; for the gaussian RMT complexity represented in blue, when in contact with the de-phasing parameter, its complexity growth (in red) has a shortened peak and a greater

downward slope that reaches plateau at later times. The non-gaussian RMT complexity illustrated by the orange plot, when interacting with white noise, reaches a downward slope instead, with saturation also occurring much later (purple). The suppressed growth of complexity witnessed from these results support those found by [14, 13] and further pointing to a suppression in spectral rigidity [11, 76, 48].

Comparing the complexity growth of the gaussian RMT illustrated by the blue plot to the orange and green plot that illustrate the presence of Non-gaussianity, this seems to flatten out the prominent ramp-peak feature that is seen in most gaussian RMT's, adding to the factors that reduce complexity outside of the environmental factor.

Chapter 4

CONCLUSION

4.1 Summary

The purpose of this thesis was underpinned with the aim of better understanding quantum complexity, this includes better interpretations on quantum chaos. The study on complexity, while inclusive of the literature that has so far contributed to the body of quantum complexity, also saw the introduction of a novel investigation on an open quantum system namely, the non-gaussian random matrix model affected by a dissipative factor γ.

We started with the definition of complexity - a concept commonly used in quantum information theory, we explored its usage in quantum physics and how it inspired the introduction of circuit complexity. Applying circuit complexity to a simple quantum field theory saw similar results when compared to the ratio obtained using a different definition of complexity known as complexity = volume C_v. Holographic complexity C_{holo}, more especially complexity = volume C_v is a probe that associates the maximised volume of time slices as the complexity found on the boundary with efforts of better understanding the Ads/CFT duality.

Another field theory (bosonic) was explored through the use of the Fubini-study metric to introduce another method of complexity known as the Fubini-study complexity, this form of complexity makes use of the symmetry found from the system's hamiltonian to define a metric that in turn will yield a geodesic distance from a reference to a target state which is interpreted as the systems' complexity.

Krylov complexity is another form of complexity included in the thesis that explores the quan-

tum mechanical framework under a Krylov subspace contained within the hilbert space. The basis under the krylov space was seen to be generated through the lanczos algorithm and consequently used to express and expand a time-dependent operator into complex time-dependent coefficients; a time evolution equation is typically applied to the operator to give a differential recurrence equation which, when solved, gives information regarding the evolution of the operator.

Depending on the problem at hand, we now know that Krylov complexity can be measured through different methods - from a geometric approach that analyses the system's symmetry and coherent states in order for the evolution of the operator to be geometrically expressed, to using an operator's two point function in order to attain lanczos coefficients that will be used to characterize the complexity of the system; we have also seen that instead of operator space, Krylov complexity can be probed in state space to give the spread complexity of an initial state. Summarily, in this study, the complexity growth of chaotic closed systems has been shown to exhibit generalized characteristics - linear growth that reaches maximal complexity, a plateau due to saturation followed by a Poincare recurrence.

In chapter 3, the question of complexity in open systems was investigated to which, different approaches were also investigated. Krylov complexity within open systems follows the same outline noted within the closed systems, the differentiating factor comes in when considering the system's liouvillian. The presence of linbladian operators and the non-hermiticity of the open system called for the use of the arnoldi algorithm which was used in characterizing and discerning chaotic systems through its arnoldi coefficients.

Continuing with the Linbladian, the evolution of the operator in the open system can also be expressed as a differential recurrence equation known as the tight bonding model to which when solved, is also used in defining Krylov complexity. The characterization of chaos in systems is typically noticed due to the linear growth of complexity, in the open system investigated in chapter 3.2, dissipation found in the system was attributed as the cause to the suppressed, non-linear complexity growth that was witnessed.

In Chapter 3.3 we see the use of circuit complexity in an open system with the introduction of complexity of purification, this method of complexity generalizes the concepts of pure state circuit complexity to mixed states. Applying this method to the chaos-like inverted harmonic oscillator

included the use of a pure wave function and disentangled reduced density matrix as the target state, the circuit complexity carried out also saw results corroborating with literature that support a linear growth in complexity for chaotic systems.

Chapter 3.3.1 introduced a probe that proved less sensitive to detecting the growth of complexity namely - complexity through operator state mapping method. The procedure of mapping an operator that has a matrix representation to a corresponding state without a tracing minimization is believed to be one of leading reasons as to why there's an overwhelming presence of saturation through time witnessed in the complexity growth of an inverted harmonic oscillator.

Investigating an open quantum system and its Krylov complexity through the use of a novel non-gaussian random matrix theory model, the presence of the environment modelled through a strength-de-phasing parameter brought a decrease in the growth of the state complexity that is typically witnessed in both open gaussian and open non gaussian random matrix theories, the role that non gaussianity plays has also been noted as a decreasing factor in state complexity.

4.2 Outlook

The extensiveness of the complexity literature for open quantum systems is still underway and so with more models and methodologies being explored, the better the knowledge will become in knowing the different factors that affect the growth of complexity. Continuing with the study of complexity and following [9]'s suggestions, q-complexity offers another type of complexity that goes beyond the bounds of Krylov complexity and OTOC's which is worth investigating. The geometric relation of Krylov complexity to phase space volumes through the liouvillian and coherent states as per [11] also opens new research avenues of exploring non-generalized combinations of algebra elements - drawing from [77, 78], the use of machine learning in this area would also makes for good research.

BIBLIOGRAPHY

[1] M. Elhoushi, "Modeling a quantum computer," Ph.D. dissertation, 12 2011.

[2] S. Chapman and G. Policastro, "Quantum computational complexity from quantum information to black holes and back," *The European Physical Journal C*, vol. 82, no. 2, pp. 1–40, 2022.

[3] R. Abt, "Implementing aspects of quantum information into the ads/cft correspondence," Ph.D. dissertation, 01 2019.

[4] L. Susskind, "Entanglement is not enough," 2014. [Online]. Available: https://arxiv.org/abs/1411.0690

[5] R. A. Jefferson and R. C. Myers, "Circuit complexity in quantum field theory," *Journal of High Energy Physics*, vol. 2017, no. 10, oct 2017. [Online]. Available: https://doi.org/10.1007%2Fjhep10%282017%29107

[6] V. Guifre, "Multi-scale entanglement renormalization ansatz," 2015. [Online]. Available: https://www.benasque.org/2015gravity/talks_contr/211_VidalBenasque2015.pdf

[7] T. Ali, A. Bhattacharyya, S. S. Haque, E. H. Kim, and N. Moynihan, "Time evolution of complexity: a critique of three methods," *Journal of High Energy Physics*, vol. 2019, no. 4, pp. 1–43, 2019.

[8] E. Rabinovici, A. Sánchez-Garrido, R. Shir, and J. Sonner, "Operator complexity: a journey to the edge of krylov space," *Journal of High Energy Physics*, vol. 2021, no. 6, jun 2021. [Online]. Available: https://doi.org/10.1007%2Fjhep06%282021%29062

[9] D. E. Parker, X. Cao, A. Avdoshkin, T. Scaffidi, and E. Altman, "A universal operator growth hypothesis," *Physical Review X*, vol. 9, no. 4, oct 2019. [Online]. Available: https://doi.org/10.1103%2Fphysrevx.9.041017

[10] P. Caputa, J. M. Magan, and D. Patramanis, "Geometry of krylov complexity," 2021. [Online]. Available: https://arxiv.org/abs/2109.03824

[11] V. Balasubramanian, P. Caputa, J. Magan, and Q. Wu, "Quantum chaos and the complexity of spread of states," 2022. [Online]. Available: https://arxiv.org/abs/2202.06957

[12] A. Bhattacharya, P. Nandy, P. P. Nath, and H. Sahu, "Operator growth and krylov construction in dissipative open quantum systems," 2022. [Online]. Available: https://arxiv.org/abs/2207.05347

[13] C. Liu, H. Tang, and H. Zhai, "Krylov complexity in open quantum systems," 2022. [Online]. Available: https://arxiv.org/abs/2207.13603

[14] A. Bhattacharyya, T. Hanif, S. S. Haque, and M. K. Rahman, "Complexity for an open quantum system," *Physical Review D*, vol. 105, no. 4, p. 046011, 2022.

[15] S. Ryu and T. Takayanagi, "Aspects of holographic entanglement entropy," *Journal of High Energy Physics*, vol. 2006, no. 08, p. 045, 2006.

[16] ——, "Holographic derivation of entanglement entropy from the anti–de sitter space/conformal field theory correspondence," *Physical review letters*, vol. 96, no. 18, p. 181602, 2006.

[17] M. Van Raamsdonk, "Building up space–time with quantum entanglement," *International Journal of Modern Physics D*, vol. 19, no. 14, pp. 2429–2435, 2010.

[18] S. Aaronson, "The complexity of quantum states and transformations: From quantum money to black holes," 2016. [Online]. Available: https://arxiv.org/abs/1607.05256

[19] J. Watrous, "Quantum computational complexity," 2008. [Online]. Available: https://arxiv.org/abs/0804.3401

[20] M. A. Nielsen, M. R. Dowling, M. Gu, and A. C. Doherty, "Quantum computation as geometry," *Science*, vol. 311, no. 5764, pp. 1133–1135, feb 2006. [Online]. Available: https://doi.org/10.1126%2Fscience.1121541

[21] Y. Li, X. Chen, and M. P. Fisher, "Measurement-driven entanglement transition in hybrid quantum circuits," *Physical Review B*, vol. 100, no. 13, p. 134306, 2019.

[22] M. A. Nielsen and I. Chuang, "Quantum computation and quantum information," 2002.

[23] S. Gubser, I. Klebanov, and A. Polyakov, "Gauge theory correlators from non-critical string theory," *Physics Letters B*, vol. 428, no. 1-2, pp. 105–114, may 1998. [Online]. Available: https://doi.org/10.1016%2Fs0370-2693%2898%2900377-3

[24] J. Maldacena, *International Journal of Theoretical Physics*, vol. 38, no. 4, pp. 1113–1133, 1999. [Online]. Available: https://doi.org/10.1023%2Fa%3A1026654312961

[25] S. Ryu and T. Takayanagi, "Holographic derivation of entanglement entropy from the anti–de sitter space/conformal field theory correspondence," *Physical Review Letters*, vol. 96, no. 18, may 2006. [Online]. Available: https://doi.org/10.1103%2Fphysrevlett.96.181602

[26] Y. Nomura, N. Salzetta, F. Sanches, and S. J. Weinberg, "Spacetime equals entanglement," *Physics Letters B*, vol. 763, pp. 370–374, dec 2016. [Online]. Available: https://doi.org/10.1016%2Fj.physletb.2016.10.045

[27] T. Hartman and J. Maldacena, "Time evolution of entanglement entropy from black hole interiors," *Journal of High Energy Physics*, vol. 2013, no. 5, pp. 1–28, 2013.

[28] D. Stanford and L. Susskind, "Complexity and shock wave geometries," *Physical Review D*, vol. 90, no. 12, dec 2014. [Online]. Available: https://doi.org/10.1103%2Fphysrevd.90.126007

[29] A. R. Brown, D. A. Roberts, L. Susskind, B. Swingle, and Y. Zhao, "Complexity, action, and black holes," *Physical Review D*, vol. 93, no. 8, apr 2016. [Online]. Available: https://doi.org/10.1103%2Fphysrevd.93.086006

[30] J. Couch, W. Fischler, and P. H. Nguyen, "Noether charge, black hole volume, and complexity," *Journal of High Energy Physics*, vol. 2017, no. 3, mar 2017. [Online]. Available: https://doi.org/10.1007%2Fjhep03%282017%29119

[31] G. Evenbly and G. Vidal, "Tensor network renormalization yields the multiscale entanglement renormalization ansatz," *Physical Review Letters*, vol. 115, no. 20, nov 2015. [Online]. Available: https://doi.org/10.1103%2Fphysrevlett.115.200401

[32] B. Swingle, "Entanglement renormalization and holography," *Physical Review D*, vol. 86, no. 6, sep 2012. [Online]. Available: https://doi.org/10.1103%2Fphysrevd.86.065007

[33] J. Jiang, Z. Chen, and C. Liu, "Switchback effect of holographic complexity in multiple-horizon black holes," *Eur. Phys. J. C*, vol. 80, no. 4, p. 306, 2020.

[34] D. Carmi, R. C. Myers, and P. Rath, "Comments on holographic complexity," *Journal of High Energy Physics*, vol. 2017, no. 3, mar 2017. [Online]. Available: https://doi.org/10.1007%2Fjhep03%282017%29118

[35] S. Chapman, J. Eisert, L. Hackl, M. P. Heller, R. Jefferson, H. Marrochio, and R. C. Myers, "Complexity and entanglement for thermofield double states," *SciPost Physics*, vol. 6, no. 3, mar 2019. [Online]. Available: https://doi.org/10.21468%2Fscipostphys.6.3.034

[36] M. A. Nielsen, "A geometric approach to quantum circuit lower bounds," 2005. [Online]. Available: https://arxiv.org/abs/quant-ph/0502070

[37] P. Bueno, J. M. Magan, and C. S. Shahbazi, "Complexity measures in qft and constrained geometric actions," 2019. [Online]. Available: https://arxiv.org/abs/1908.03577

[38] S. Chapman, M. P. Heller, H. Marrochio, and F. Pastawski, "Toward a definition of complexity for quantum field theory states," *Physical Review Letters*, vol. 120, no. 12, mar 2018. [Online]. Available: https://doi.org/10.1103%2Fphysrevlett.120.121602

[39] A. Perelomov, "Coherent states for arbitrary lie groups," *Journal of High Energy Physics*, vol. 26, no. 222. [Online]. Available: https://doi.org/10.1007/BF01645091,year=1972,month={nov},publisher={CommunicationsinMathematicalPhysics.}

[40] A. N. Krylov, "On the numerical solution of the equation by which in technical questions frequencies of small oscillations of material systems are determined," *Izvestija AN SSSR (News of Academy of Sciences of the USSR), Otdel. mat. i estest. nauk*, vol. 7, no. 4, pp. 491–539, 1931.

[41] S. Fan, "An introduction to krylov subspace methods," 2018. [Online]. Available: https://arxiv.org/abs/1811.09025

[42] M. Srednicki, "The approach to thermal equilibrium in quantized chaotic systems," *Journal of Physics A: Mathematical and General*, vol. 32, no. 7, pp. 1163–1175, jan 1999. [Online]. Available: https://doi.org/10.1088%2F0305-4470%2F32%2F7%2F007

[43] V. Viswanath and G. Muller, *The recursion method*, ser. Lecture Notes in Physics Monographs, 23. Berlin, Heidelberg : Springer Berlin Heidelberg, 1994.

[44] J. L. F. Barbón, E. Rabinovici, R. Shir, and R. Sinha, "On The Evolution Of Operator Complexity Beyond Scrambling," *JHEP*, vol. 10, p. 264, 2019.

[45] J. Sonner and M. Vielma, "Eigenstate thermalization in the sachdev-ye-kitaev model," *Journal of High Energy Physics*, vol. 2017, no. 11, nov 2017. [Online]. Available: https://doi.org/10.1007%2Fjhep11%282017%29149

[46] T. Hartman and J. Maldacena, "Time evolution of entanglement entropy from black hole interiors," *Journal of High Energy Physics*, vol. 2013, no. 5, may 2013. [Online]. Available: https://doi.org/10.1007%2Fjhep05%282013%29014

[47] O. Bohigas, M.-J. Giannoni, and C. Schmit, "Characterization of chaotic quantum spectra and universality of level fluctuation laws," *Physical review letters*, vol. 52, no. 1, p. 1, 1984.

[48] F. J. Dyson, "Statistical theory of the energy levels of complex systems. i," *Journal of Mathematical Physics*, vol. 3, no. 1, pp. 140–156, 1962.

[49] I. Dumitriu and A. Edelman, "Matrix models for beta ensembles," *Journal of Mathematical Physics*, vol. 43, no. 11, pp. 5830–5847, nov 2002. [Online]. Available: https://doi.org/10.1063%2F1.1507823

[50] H.-P. Breuer, F. Petruccione *et al.*, *The theory of open quantum systems*. Oxford University Press on Demand, 2002.

[51] H. Carmichael, *An open systems approach to quantum optics: lectures presented at the Université Libre de Bruxelles, October 28 to November 4, 1991*. Springer Science & Business Media, 2009, vol. 18.

[52] C. Gardiner, P. Zoller, and P. Zoller, *Quantum noise: a handbook of Markovian and non-Markovian quantum stochastic methods with applications to quantum optics*. Springer Science & Business Media, 2004.

[53] A. Rivas and S. F. Huelga, *Open quantum systems*. Springer, 2012, vol. 10.

[54] G. Lindblad, "On the generators of quantum dynamical semigroups," *Communications in Mathematical Physics*, vol. 48, no. 2, pp. 119–130, 1976.

[55] Aug 1976. [Online]. Available: https://doi.org/10.1063/1.522979

[56] Bindel, "Matrix computations (cs 6210)," November 2016, [Online; posted 16-November-2016]. [Online]. Available: https://www.cs.cornell.edu/~bindel/class/cs6210-f16/lec/2016-11-16.pdf

[57] G. Akemann, M. Kieburg, A. Mielke, and T. Prosen, "Universal signature from integrability to chaos in dissipative open quantum systems," *Physical Review Letters*, vol. 123, no. 25, dec 2019. [Online]. Available: https://doi.org/10.1103%2Fphysrevlett.123.254101

[58] W. Dür and H. J. Briegel, "Entanglement purification and quantum error correction," *Reports on Progress in Physics*, vol. 70, no. 8, p. 1381, 2007.

[59] C. A. Agón, M. Headrick, and B. Swingle, "Subsystem complexity and holography," *Journal of High Energy Physics*, vol. 2019, no. 2, pp. 1–55, 2019.

[60] W. Unruh and W. H. Zurek, "Reduction of a wave packet in quantum brownian motion," *Physical Review D*, vol. 40, no. 4, p. 1071, 1989.

[61] E. Caceres, S. Chapman, J. D. Couch, J. P. Hernandez, R. C. Myers, and S.-M. Ruan, "Complexity of mixed states in qft and holography," *Journal of High Energy Physics*, vol. 2020, no. 3, pp. 1–120, 2020.

[62] A. Bhattacharyya, T. Takayanagi, and K. Umemoto, "Entanglement of purification in free scalar field theories," *Journal of High Energy Physics*, vol. 2018, no. 4, pp. 1–28, 2018.

[63] A. Bhattacharyya, A. Jahn, T. Takayanagi, and K. Umemoto, "Entanglement of purification in many body systems and symmetry breaking," *Physical review letters*, vol. 122, no. 20, p. 201601, 2019.

[64] T. Ali, A. Bhattacharyya, S. S. Haque, E. H. Kim, N. Moynihan, and J. Murugan, "Chaos and complexity in quantum mechanics," *Physical Review D*, vol. 101, no. 2, p. 026021, 2020.

[65] M.-D. Choi, "Completely positive linear maps on complex matrices," *Linear algebra and its applications*, vol. 10, no. 3, pp. 285–290, 1975.

[66] A. Jamiołkowski, "Linear transformations which preserve trace and positive semidefiniteness of operators," *Reports on Mathematical Physics*, vol. 3, no. 4, pp. 275–278, 1972.

[67] A. Gaikwad and R. Sinha, "Spectral form factor in non-gaussian random matrix theories," *Physical Review D*, vol. 100, no. 2, p. 026017, 2019.

[68] E. Bré zin and S. Hikami, "Spectral form factor in a random matrix theory," *Physical Review E*, vol. 55, no. 4, pp. 4067–4083, apr 1997. [Online]. Available: https://doi.org/10.1103%2Fphysreve.55.4067

[69] J. S. Cotler, G. Gur-Ari, M. Hanada, J. Polchinski, P. Saad, S. H. Shenker, D. Stanford, A. Streicher, and M. Tezuka, "Black holes and random matrices," *Journal of High Energy Physics*, vol. 2017, no. 5, pp. 1–54, 2017.

[70] E. Dyer and G. Gur-Ari, "2d cft partition functions at late times," *Journal of High Energy Physics*, vol. 2017, no. 8, pp. 1–35, 2017.

[71] Z. Xu, A. Chenu, T. Prosen, and A. del Campo, "Thermofield dynamics: Quantum chaos versus decoherence," *Physical Review B*, vol. 103, no. 6, p. 064309, 2021.

[72] J. Cornelius, Z. Xu, A. Saxena, A. Chenu, and A. Del Campo, "Spectral filtering induced by non-hermitian evolution with balanced gain and loss: Enhancing quantum chaos," *Physical Review Letters*, vol. 128, no. 19, p. 190402, 2022.

[73] A. S. Matsoukas-Roubeas, F. Roccati, J. Cornelius, Z. Xu, A. Chenu, and A. del Campo, "Non-hermitian hamiltonian deformations in quantum mechanics," *Journal of High Energy Physics*, vol. 2023, no. 1, pp. 1–31, 2023.

[74] M. Hayashi, S. Ishizaka, A. Kawachi, G. Kimura, and T. Ogawa, *Introduction to quantum information science*. Springer, 2014.

[75] E. Brézin and A. Zee, "Universality of the correlations between eigenvalues of large random matrices," *Nuclear Physics B*, vol. 402, no. 3, pp. 613–627, 1993.

[76] M. L. Mehta, "On the statistical properties of the level-spacings in nuclear spectra," *Nuclear Physics*, vol. 18, pp. 395–419, 1960.

[77] J. López García and Á. Rivero, "Phase space learning with neural networks," in *Advances on Links Between Mathematics and Industry: CTMI 2019*. Springer, 2021, pp. 131–152.

[78] L. Kong, Y. Chen, and M. Zhang, "Geodesic graph neural network for efficient graph representation learning," *arXiv preprint arXiv:2210.02636*, 2022.